Funded by
the European Union

Project Title:

Eco-operated, Modular, highly efficient, and flexible multi-POWERtrain for long-haul heavy-duty vehicles

Acronym: EMPOWER

Grant Agreement No.: 101096028

Topic:	**Report on energy conversion systems testing [M4-M28]**
Topic identifier:	**HORIZON-CL5-2022-D5-01-08**
Type of action:	**Innovation Action (IA)**

Deliverable No.	D2.3	
Deliverable Title	Report on energy conversion systems testing	
Deliverable Date	2025-04	
Deliverable Type	Report	
Dissemination level	Public	
Written by	Michele MICCIO (FPT) Imad MATRAJI (FMF) Leonidas TSIKONIS (FMF) Giacomo MANCA DI VILLAHERMOSA (FMF) Niklas GUENTERT (FMF) Michael STRIEDNIG (FMF) Leonardo CHIACCHIARARELLI (FMF) Francesco LAZZARINI (FPT) David Donatello D'AMATO (FPT) Filippo COSTA (FPT) Stefano ALBANELLO (FPT)	2025-02-02 to 2025-04-29
Checked by	Manasa SRIDHAR (FMF) Dragan SIMIC (AIT) Claudio MEZZA (IVECO)	2025-04-29 to 2025-05-16

This project has received funding from the European Union's HORIZON EUROPE research and innovation programme under grant agreement No. 101096028. The content of this publication is the sole responsibility of the Consortium partners listed herein and does not necessarily represent the view of the European Commission or its services.

	Jokin BATALLA (CID) Thomas BÄUML (AIT)	
Approved by	Michele MICCIO (FPT) Luca GIOVENZANA (FMF) Samanta VALSANIA (FPT)	2025-05-16
Status	Version 1.0 Version 2.0 Version 3.0 Version 4.0	2025-02-24 2025-04-29 2025-05-07 2025-05-16

This project has received funding from the European Union's HORIZON EUROPE research and innovation programme under grant agreement No. 101096028. The content of this publication is the sole responsibility of the Consortium partners listed herein and does not necessarily represent the view of the European Commission or its services.

Publishable Executive Summary

The EMPOWER project is focused on developing two modular, flexible zero-emission heavy-duty vehicles (ZE HDVs) in the VECTO Group 9 category, each with a gross vehicle weight (GVW) of at least 40 tons and reaching Technology Readiness Level (TRL) 8. The two vehicle types include:

- A Fuel Cell Electric Vehicle (FCEV) optimized for long-haul operations, offering a range of up to 750 km without refueling.
- A Battery Electric Vehicle (BEV) tailored for regional distribution, with a maximum range of 400 km on a single charge.

The project prioritizes modularity, scalability, and cost-effectiveness, aiming to ensure high performance, manufacturability, and user acceptance. Central to achieving competitive vehicle solutions are the eAxle and Fuel Cell system, both of which are crucial to meeting EU CO_2 targets, depending on market uptake and sales volumes.

This document details the validation efforts conducted under Work Package 2 (WP2), focusing on the development and testing of the eAxle and Fuel Cell system. For both components, the validation includes:

- Component-level testing
- Embedded software commissioning and calibration
- Functional validation
- Durability and design verification testing (DVP)

Specific test methodologies include structural, lubrication, environmental, durability, and differential lock tests for the eAxle, as well as system integration and performance assessments for the Fuel Cell system.

This project has received funding from the European Union's HORIZON EUROPE research and innovation programme under grant agreement No. 101096028. The content of this publication is the sole responsibility of the Consortium partners listed herein and does not necessarily represent the view of the European Commission or its services.

Table of Contents

This project has received funding from the European Union's HORIZON EUROPE research and innovation programme under grant agreement No. 101096028. The content of this publication is the sole responsibility of the Consortium partners listed herein and does not necessarily represent the view of the European Commission or its services.

List of Figures

This project has received funding from the European Union's HORIZON EUROPE research and innovation programme under grant agreement No. 101096028. The content of this publication is the sole responsibility of the Consortium partners listed herein and does not necessarily represent the view of the European Commission or its services.

List of Tables

Abbreviations and Nomenclature

Table 1: Abbreviations and Nomenclatures

Symbol or Short name	Description
ADC	Amperes Direct Current
ASIL	Automotive Safety Integrity Level
BEV	Battery Electric Vehicle
BMS	Battery Management System
Cab	Cabin
CAD	Computer Aided Design
DC	Direct Current
DC/DC	Direct Current to Direct Current Converter
EMC	Electromagnetic Compatibility
EV	Electrical Vehicle
e-VECOP	Electrified Vehicle Control Platform
FCCU	Fuel Cell Control Unit

This project has received funding from the European Union's HORIZON EUROPE research and innovation programme under grant agreement No. 101096028. The content of this publication is the sole responsibility of the Consortium partners listed herein and does not necessarily represent the view of the European Commission or its services.

Symbol or Short name	Description
FCEV	Fuel Cell Electric Vehicle
FCS	Fuel cell system
FP	Full Pneumatic
FTA	Fault Tree Analysis
GCW	Gross Combination Weight
GVW	Gross Vehicle Weight
HDV	Heavy-Duty Vehicles
HS	High Side of the DC/DC converter
HSS	Hydrogen Storage System
HV	High Voltage
HVAC	Heating, Ventilation and Air Conditioning
HVI	Human Vehicle Interaction
HW	Hardware
IG	Iveco Group
IGBT	Insulated-gate bipolar transistor
IMD	Isolation Monitoring Device
IPMSM	Interior Permanent Magnet Synchronous Machine
IVG	Iveco Group
LCA	Life Cycle Assessment
LCV	Light Commercial Vehicle
LS	Low Side of the DC/DC converter
LV	Low Voltage
MBD	Model Based Development
MD	Medium-Duty
P	Pneumatic
PDU	Power Distribution Unit
PTO	Power take off
SiC	Silicon Carbide
SOC	State of charge
SW	Software
TCO	Total Cost of Operation
TMS	Thermal management system
TRL	Technology Readiness Level
UC	Use-Case
V2G	Vehicle-to-Grid
VCU	Vehicle Control Unit

This project has received funding from the European Union's HORIZON EUROPE research and innovation programme under grant agreement No. 101096028. The content of this publication is the sole responsibility of the Consortium partners listed herein and does not necessarily represent the view of the European Commission or its services.

Symbol or Short name	Description
VDC	Volt Direct Current
VECTO	Vehicle Energy Consumption Calculation Tool
VP	Iveco vehicle identification code
WP	Work Package
ZE-HDV	Zero-Emission Heavy-Duty Vehicles
ZEV	Zero Emission Vehicle

This project has received funding from the European Union's HORIZON EUROPE research and innovation programme under grant agreement No. 101096028. The content of this publication is the sole responsibility of the Consortium partners listed herein and does not necessarily represent the view of the European Commission or its services.

1 Introduction

In 2020 the CO_2 emissions of the transport sector in the EU-27 accounted for approximately 27 % of the total emissions [1]. Thereof about 5.6 % are produced by Heavy Duty Vehicles (HDVs) and buses [2]. However, the year 2020 is, due to COVID-19 related restrictions and lockdowns and therefore altered mobility patterns, not very representative. Analyses of the last months in 2020 show that road transport activity was expected to recover to pre-COVID-19 levels in 2021, with CO_2 emissions rising to just 5 % below the 2019 level [3]. Therefore, this sector calls for a massive shift to zero tailpipe emissions to achieve full carbon neutrality by 2050. A study conducted by the European Automobile Manufacturers' Association (ACEA) found out, that in 2020 about 6.2 million medium and heavy-duty commercial vehicles were on the EU's roads [4]. Approximately 96.3 % of these trucks ran on diesel fuel, 0.7 % on petrol and only 0.24 % were zero-emission, providing potential for the transformation of the transport sector to ZE HDVs to reach carbon neutrality by 2050.

The objective of EMPOWER is to deliver two modular and flexible ZE HDVs of VECTO group 9 with a GVW of at least 40 tons, both at TRL 8 level:

- a Fuel Cell Electric Vehicle (FCEV), suitable for long-haul operation conditions with a maximum unrefuelled range of 750 km;
- a Battery Electric Vehicle (BEV) vehicle, designed for regional distribution mission profiles with a maximum un-recharged driving range of 400 km.

The **ambition of EMPOWER** involves the development, implementation, and demonstration of these vehicles at TRL 8, guaranteeing a maximum load capacity of not less than 90 %. They will be compared to conventional trucks of the same vehicle class, making them ready to enter the market in 2029 with equal Total Cost of Ownership (TCO) as 2020 engine-based solutions, assuming a production volume of more than 10,000 vehicles/year.

A particular attention will be focused on:

- **Modularity,** between different vehicles with specific electrification technology.
- **Scalability** of content under development with possible integration into other applications (even outside project perimeter).
- **Competitiveness** of product and technology in terms of performance, cost, automotive manufacturing, customer acceptance.

The eAxle and the Fuel Cell system were two of the main products identified as critical contributors to the achievement of competitive BEV and FCEV vehicles to help achieve the EU CO_2-targets, depending on customer acceptance and sales volumes. This document is the follow up to D2.1 and D2.2 and describes the validation campaigns performed on these vehicle sub-systems.

1.1 Scope and objectives

The aim of this document is to present and describe the deliverables of Task 2.3 and Task 2.4 consisting of the validation campaigns of the eAxle and the Fuel Cell system developed within the framework of WP2, specifically in Task 2.1 and Task 2.2; the detailed description of the systems and design objectives and results is part of D2.1 and D2.2, therefore the focus on this document will be on the validation plan and description of the results.

This project has received funding from the European Union's HORIZON EUROPE research and innovation programme under grant agreement No. 101096028. The content of this publication is the sole responsibility of the Consortium partners listed herein and does not necessarily represent the view of the European Commission or its services.

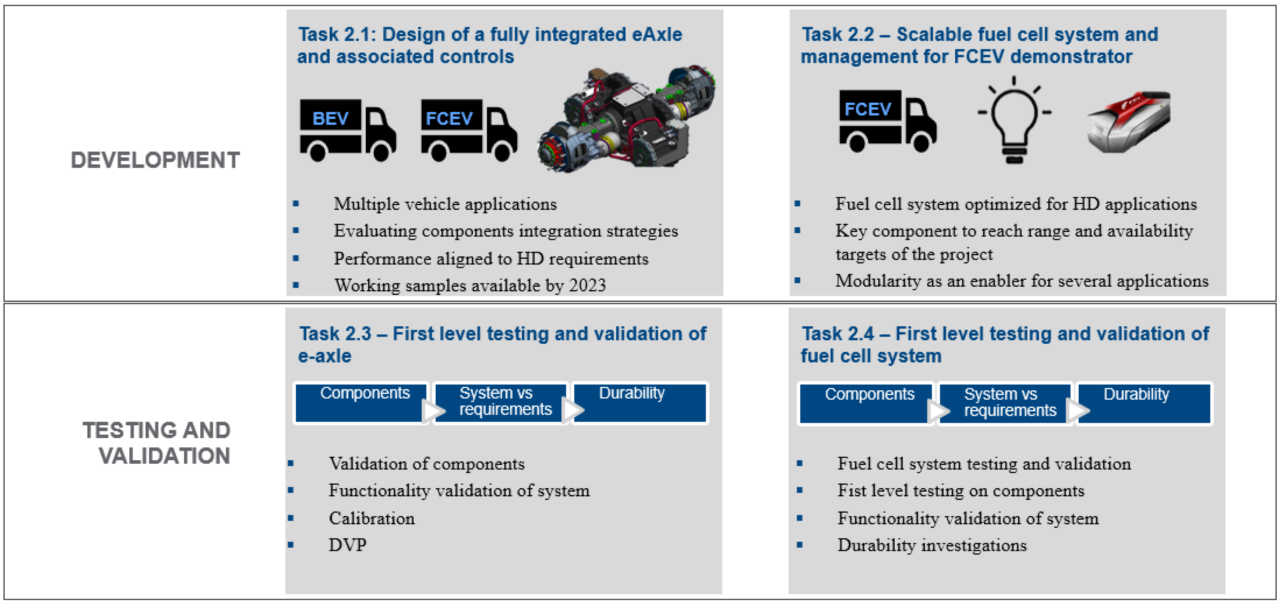

Figure 1: Overview of Tasks in WP2.

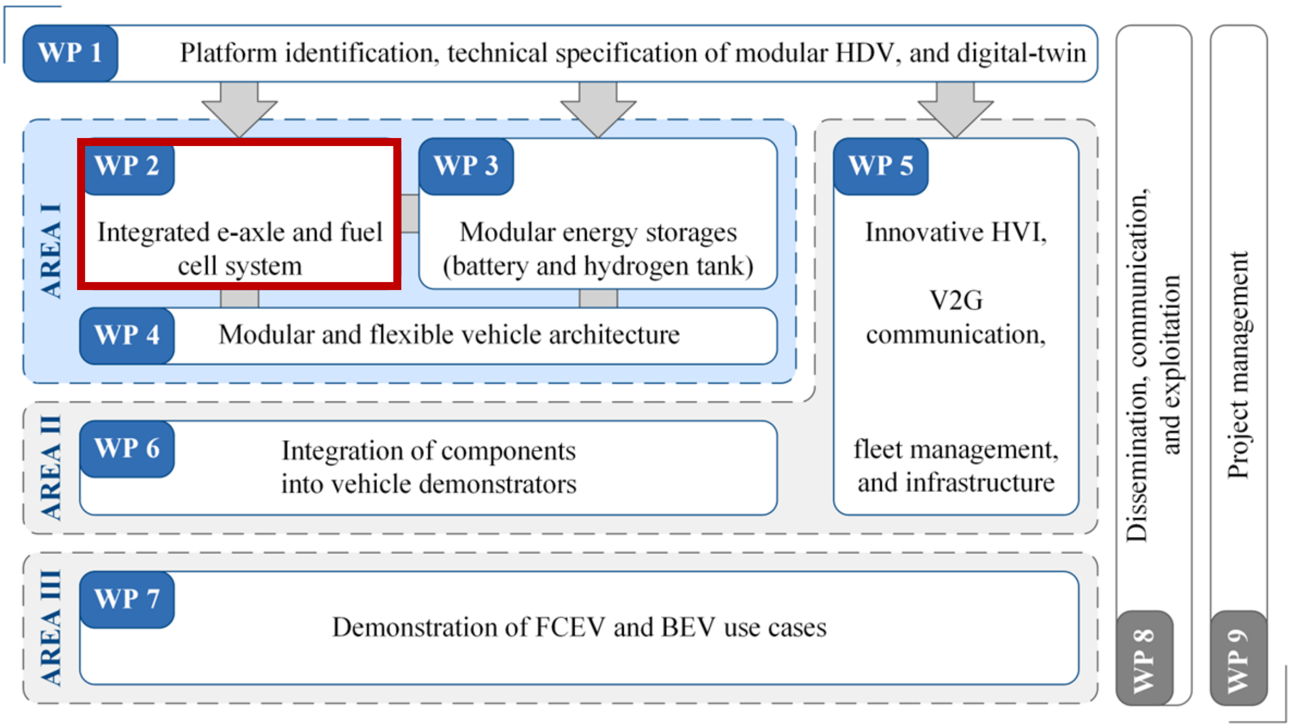

Figure 2: EMPOWER work packages diagram.

The presented solutions are based on the fulfilment of the nine main objectives of EMPOWER (see Figure 3), moreover, the defined vehicle platform allows the installation of modular (Battery Electric or FC-Electric) powertrain solutions, exploiting the scalability and modularity of the installed power units. This aspect allows cost efficient solutions for any kind of dedicated mission.

This project has received funding from the European Union's HORIZON EUROPE research and innovation programme under grant agreement No. 101096028. The content of this publication is the sole responsibility of the Consortium partners listed herein and does not necessarily represent the view of the European Commission or its services.

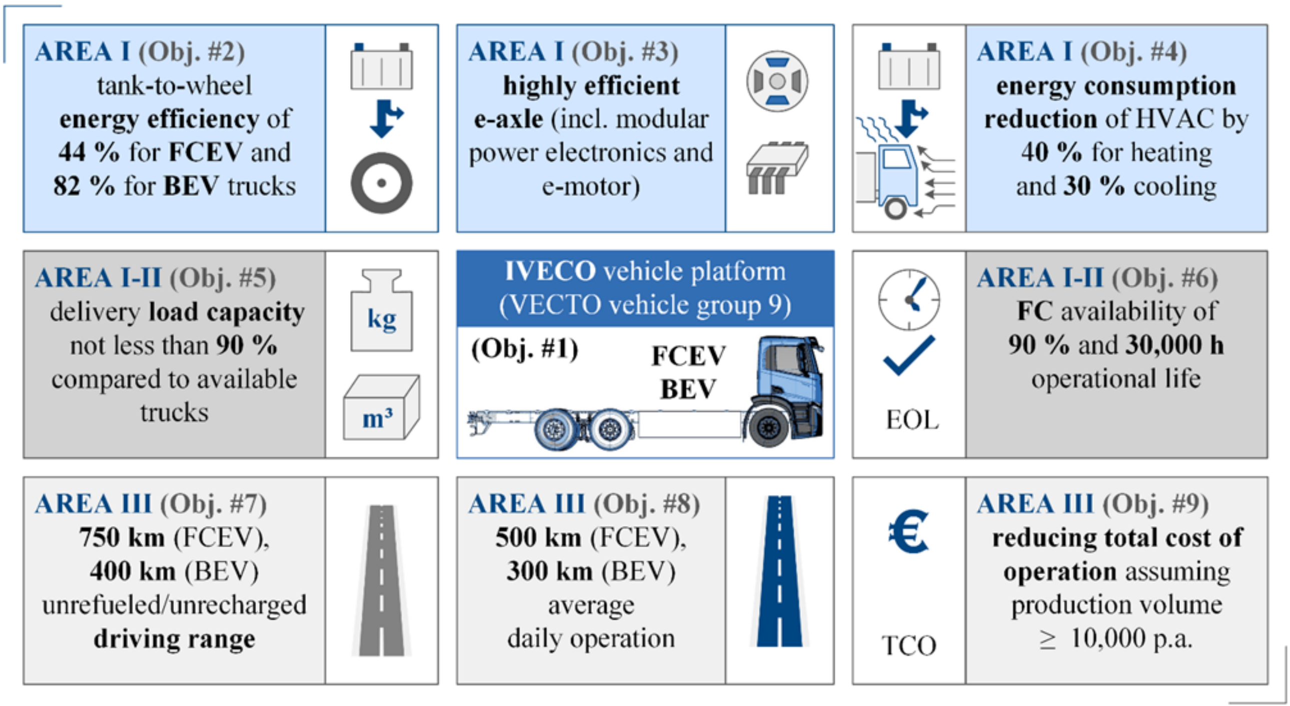

Figure 3: Nine EMPOWER objectives.

EMPOWER has three AREAs in which its activities take place. AREAs I and II develop the modular and scalable vehicle concept, a highly efficient e-axle, an electric braking energy recovery system, an efficient HVAC system based on the refrigerant CO_2 combined with infrared panels for efficient cabin heating, and an innovative HVI that provides functionalities like eco-routing and predictive maintenance.

AREA III deals with the six-month demonstration of the FCEV and BEV demonstrators at TRL 8, making the EMPOWER technology ready to reach the market by 2029.

Nine main objectives have been identified and separated into several distinctive key features developed in EMPOWER.

This project has received funding from the European Union's HORIZON EUROPE research and innovation programme under grant agreement No. 101096028. The content of this publication is the sole responsibility of the Consortium partners listed herein and does not necessarily represent the view of the European Commission or its services.

Table 2: EMPOWER objectives and KPIs.

Topics	SotA 2022	KPIs	EMPOWER target	AREA	EMPOWER key features (contributing to the specific objective)	Target TRL	Demonstrator platform
FCEV and BEV demonstrators **(Obj. #1)**	diesel long-haul and regional distribution vehicles	↑	zero-emission long-haul and regional distribution vehicles	I	re-designed and innovative components, modularity, and digital twin models	TRL 8	FCEV & BEV
				II	new improved HVI, eco-routing and assistance, V2G communication	TRL 7	
				III	demonstrators (FCEV and BEV) and corresponding LCA of the vehicles	TRL 8	
tank-to-wheel energy efficiency **(Obj. #2)**	40 % for FCEV[1] 70 % for BEV[2]	+4 % +12 %	44 % for FCEV 82 % for BEV	I	FC continuous power 250 – 300 kW	TRL 7	FCEV
				I	next-generation power electronics		FCEV & BEV
				I	e-motor continuous power 350 – 540 kW[3]		FCEV & BEV
				I	integrated and efficient multi-speed transmission		FCEV & BEV
efficiency and modularity of e-axle **(Obj. #3)**	95 % peak efficiency[1]	+1.5 %	96.5 % peak efficiency	I	functionally integrated e-motor combined with modular electrified braking system	TRL 8	FCEV & BEV
				I	improved power electronic solution		
HVAC system power **(Obj. #4)**	5 kW heating 8 kW cooling	-40 % -30 %	3 kW heating 5.6 kW cooling	I	infrared radiative panels	TRL 7	FCEV & BEV
				I	CO_2-based HVAC system		
				I	thermal insulation and optimised energy management of the truck cabin		
delivery load capacity **(Obj. #5)**	100 %	≤ -10 %	≥ 90 %	I-II	verify targeted delivery load capacity of ≥ 90 % compared to SotA vehicles	TRL 8	FCEV & BEV
operation lifetime of FC **(Obj. #6)**	20,000 hrs[4]	+50 %	30,000 hrs	I-II	testing and verification of FC operational life for a safe and efficient operation under real-life driving conditions	TRL 7	FCEV
maximum driving range **(Obj. #7)**	400 km[5]	+87 %	750 km FCEV	III	unrefuelled maximum driving ranges	TRL 8	FCEV
	300 km[6]	+33 %	400 km BEV	III	unrecharged maximum driving ranges		BEV

This project has received funding from the European Union's HORIZON EUROPE research and innovation programme under grant agreement No. 101096028. The content of this publication is the sole responsibility of the Consortium partners listed herein and does not necessarily represent the view of the European Commission or its services.

Topics	SotA 2022	KPIs	EMPOWER target	AREA	EMPOWER key features (contributing to the specific objective)	Target TRL	Demonstrator platform
daily average driving range **(Obj. #8)**	n.a.		500 km FCEV	III	500 km average daily driving range in real-world long-haul mission	TRL 8	FCEV
			300 km BEV	III	300 km average daily driving range in real-world regional distribution mission		BEV
total cost of operation **(Obj. #9)**	Diesel 2020 long-haul 2.4 ct/tkm Diesel 2020 reg. Distr. 2.5 ct/tkm	FCEV -15.6 % BEV -26.4 %	FCEV 2.0 ct/tkm BEV 1.8 ct/tkm	III	TCO reduction analysis of demonstrators assuming a mass production volume of ≥ 10.000 vehicles/year	n.a.	FCEV & BEV

This project has received funding from the European Union's HORIZON EUROPE research and innovation programme under grant agreement No. 101096028. The content of this publication is the sole responsibility of the Consortium partners listed herein and does not necessarily represent the view of the European Commission or its services.

1.2 Timeline

The following timeline (Table 3) focuses on WP2 and its Tasks, showing how they are located with respect to the entire program. Task 2.1 and Task 2.2 are completed, and they are instrumental for the execution of Tasks 2.3 and 2.4; Task 2.1 is described in the deliverable report D2.1 while Task 2.2 in D2.2.

Task 2.3 consists in the first level testing and validation of e-axle and Task 2.4 consists of first level testing and validation of fuel cell system; both activities started in 2023 and are the object of this document (D2.3), planned for April 2025.

Table 3: Project timing status.

WP / Task leader	EMPOWER gantt chart	Year:	2023				2024				2025				2026			
		Project quarter:	Q1	Q2	Q3	Q4	Q5	Q6	Q7	Q8	Q9	Q10	Q11	Q12	Q13	Q14	Q15	Q16
FPT	WP2	Integrated e-axle and fuel cell system																
FPT	Task 2.1	Design of fully integrated e-axle and associated controls																
FMF	Task 2.2	Scalable fuel cell system and - management for FCEV demonstrator																
FMF	Task 2.3	First level testing and validation of e-axle																
FMF	Task 2.4	First level testing and validation of fuel cell system																

1.3 Methodology

1.3.1 eAxle testing methodology

The testing and validation process of an electrified axle (eAxle) for heavy-duty (HD) vehicles is a rigorous, multi-phase approach designed to ensure performance, safety, and durability under real-world operating conditions (Figure 4). The process begins at component level and advances through integration, software commissioning, system validation, and long-term durability trials.

1. Component-Level Testing

Each major subsystem—traction motor, inverter, lubrication system, transmission gears, gear shift actuator and transmission control unit—is first tested independently. The motor undergoes dynamometer testing to validate torque, speed, and thermal performance. The inverter is subjected to power cycling and efficiency mapping under varying load profiles. Lubrication system components (electric coil pump, sensors) are characterized to verify and properly calibrate cooling and lubrication system and control logic. Gear and transmission components are analysed for backlash, NVH (noise, vibration, harshness), and mechanical robustness under high torque loads. The gear shift system is characterized in terms of actuation performances, response time and calibrated properly, The transmission control unit (TCU) is verified for logic accuracy, response time, and CAN communication integrity.

2. Embedded Software Commissioning and Calibration

Once components pass individual qualification, the embedded software is commissioned in the integrated system. Calibration includes tuning torque delivery, thermal thresholds, motor-inverter synchronization, and shift logic in the transmission. Safety interlocks and diagnostics are also validated in this phase. This is performed both in hardware-in-the-loop (HIL) environments and, later, on full system test benches to simulate real drive cycles.

3. Functional Validation

This project has received funding from the European Union's HORIZON EUROPE research and innovation programme under grant agreement No. 101096028. The content of this publication is the sole responsibility of the Consortium partners listed herein and does not necessarily represent the view of the European Commission or its services.

The fully integrated eAxle is then validated functionally on system-level test benches and prototype vehicles. This includes validating torque split, energy recovery, gear shifting and differential lock engagement. The control strategies are fine-tuned for performance and driveability.

4. Durability and Design Verification Testing (DVP)

To ensure longevity, the system undergoes extensive DVP testing. Thermal cycling tests expose the system to extreme temperature variations to check material expansion, connector reliability, and thermal fatigue. Lubrication testing verifies oil circulation, thermal dissipation, and degradation resistance under high-speed and high-load conditions. Full e-axle is tested through Endurance test, designed to reproduce aging resulting from vehicle typical mission and field operation. The differential lock mechanism is tested repeatedly under load to ensure mechanical integrity and responsiveness over the vehicle's expected life cycle.

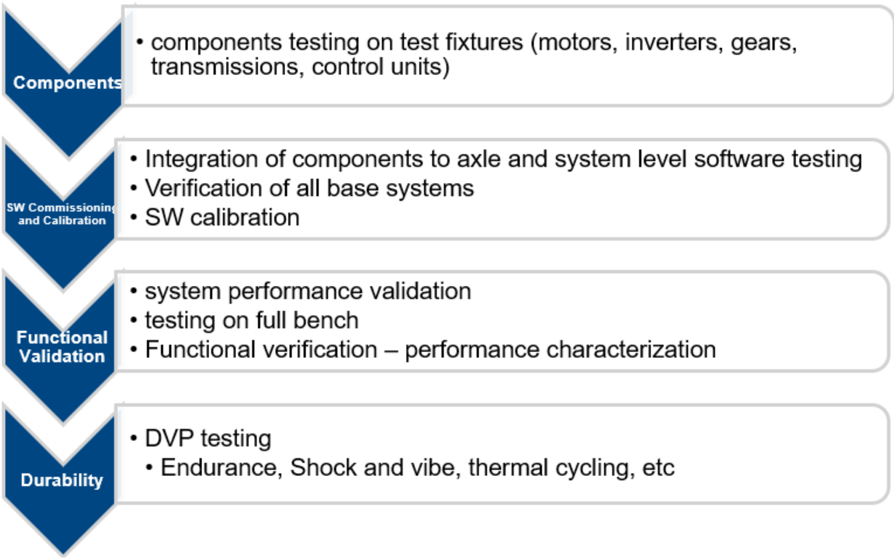

Figure 4: Validation process for eAxle in EMPOWER project.

This systematic, step-by-step approach ensures that the electrified axle meets or exceeds OEM and regulatory standards, delivering reliable performance under the demanding conditions typical of heavy-duty vehicle operations.

1.3.2 Fuel Cell System Testing and Validation Methodology

The testing and validation of a fuel cell system for heavy-duty (HD) vehicles is a critical phase in ensuring reliability, performance, and compliance with operational demands (Figure 5). This rigorous process begins with component-level validation and culminates in full-system endurance and dynamic validation. Below is a step-by-step outline of this comprehensive approach.

1. Component-Level Testing

Each subsystem and component is first evaluated individually under controlled conditions. The electric turbocharger is tested for speed response, efficiency, and thermal performance. Pumps and the DC/DC converter undergo load cycling and thermal stress validation. Fuel cell stacks are characterized for voltage-current behaviour and uniformity. Valves, humidifiers, water charge air coolers (WCAC), water separators, and ion exchangers are subjected to flow and environmental durability tests. The hydrogen injector and ejector are calibrated for precision dosing and backpressure management. The Media Supply Unit (MSU), responsible for integrated air, water, and hydrogen management, is tested for robustness under fluctuating demands. Sensors and actuators are verified for accuracy and repeatability. The software and control unit undergo

This project has received funding from the European Union's HORIZON EUROPE research and innovation programme under grant agreement No. 101096028. The content of this publication is the sole responsibility of the Consortium partners listed herein and does not necessarily represent the view of the European Commission or its services.

Hardware-in-the-Loop (HiL) simulation to ensure signal integrity, fail-safe responses, and control strategy validation.

2. Embedded Software Commissioning and Calibration

Once individual components meet specification, the system is assembled on a dedicated test station. Here, the embedded software is commissioned. Calibration routines are executed to align sensor inputs and control outputs with physical responses. Parameters such as stack temperature control, anode recirculation, and air excess ratio are fine-tuned. Closed-loop control algorithms are verified under transient and steady-state conditions to ensure stability and responsiveness across operating ranges.

3. Functional Validation

With software integrated and calibrated, the system undergoes functional validation. This includes start-up performance, load following behaviour, hydrogen purge routines, and thermal management coordination. Safety interlocks are tested against simulated faults, ensuring proper fallback behaviour. Communication with the vehicle's CAN network is verified for robustness under load.

4. Durability and DVP Testing

The final phase focuses on Durability and cycles validation, where the system is subjected to extended operation using dynamic cycles derived from real-world HD mission profiles. This includes frequent start-stops, load cycling, and idle-to-peak power transitions. Stress factors such as humidity, and ambient temperature variations are incorporated. Critical degradation metrics—stack voltage decay, water balance drift, and hydrogen leakage—are monitored to assess long-term reliability.

Through this structured testing and validation workflow, the fuel cell system is matured to meet the demanding requirements of heavy-duty transport, ensuring safe, efficient, and durable operation in the field.

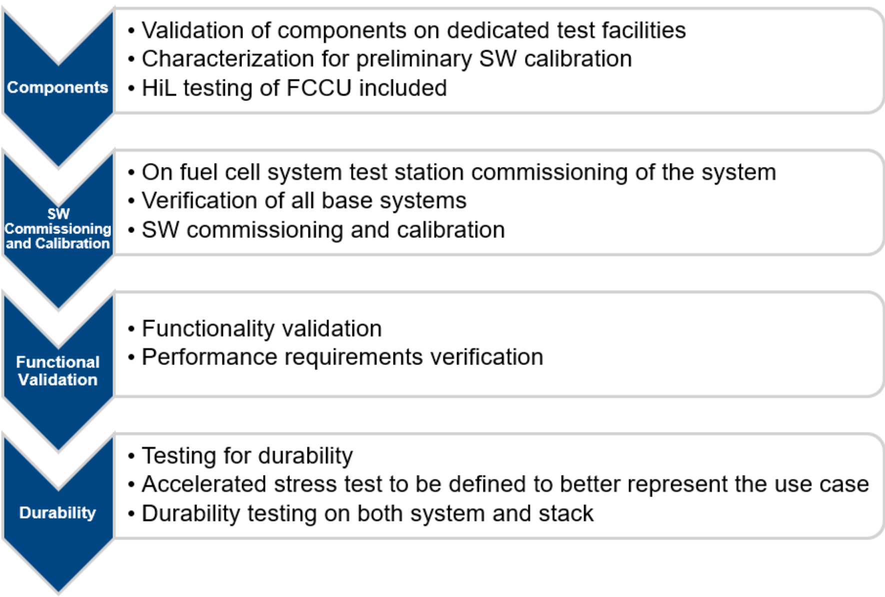

Figure 5: Validation process for Fuel Cell System.

2 First Level Testing and Validation of eAxle

In this chapter, the comprehensive testing procedures carried out to ensure the reliability and performance of the equipment are presented. These tests are designed to assess various aspects of the equipment under different

This project has received funding from the European Union's HORIZON EUROPE research and innovation programme under grant agreement No. 101096028. The content of this publication is the sole responsibility of the Consortium partners listed herein and does not necessarily represent the view of the European Commission or its services.

conditions and stress levels. The importance of these assessments lies in verifying that the products can withstand real-world operational demands and maintain optimal functionality over time.

To meet the targets, the following tests were conducted:

- Structural test
- Lubrication test
- Environmental test
- Durability test
- Differential lock test
- Gear shift test

2.1 Structural Test

2.1.1 Vertical Load Test

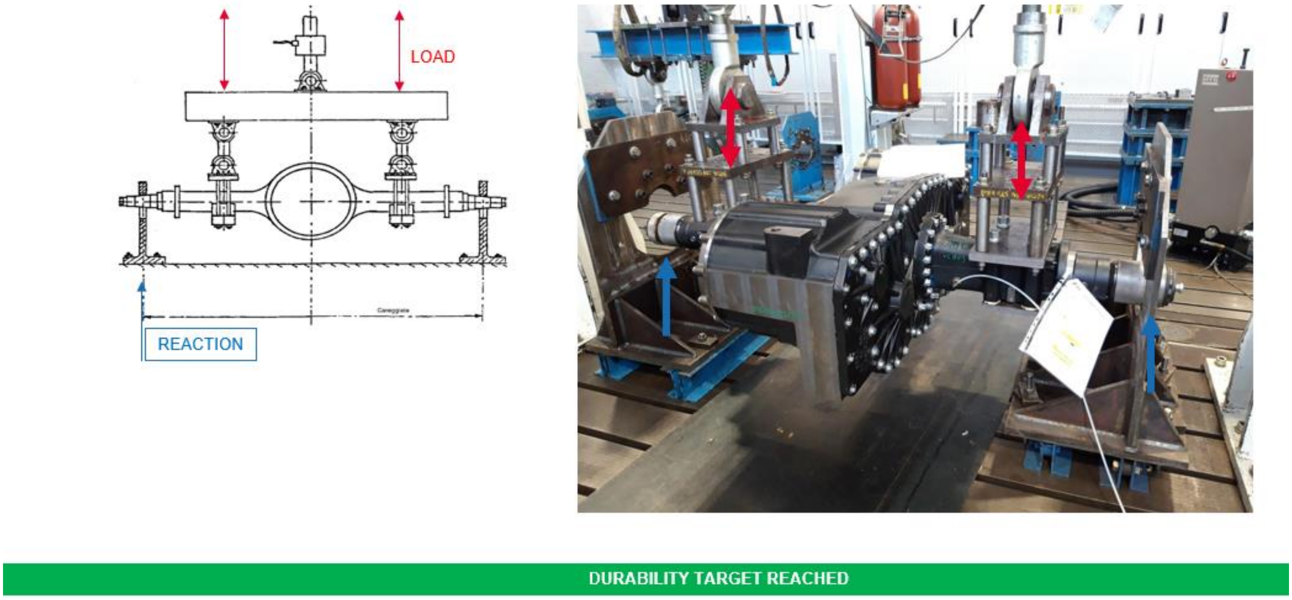

Figure 6: Structural test, vertical load.

The axle is mechanically constrained to allow the application of load in the vertical direction on the spring seats while providing a vertical reaction at the spindle points (wheel hub points). Actuators will be attached to the spring seats through an appropriate mechanical arrangement. The vertical reaction must have a free pivot degree of freedom at the spindle point along the axis parallel to the vehicle's longitudinal direction.

A cyclic load ranging from 0 to appropriate Load (based on static operating payload and relative safety factor to take account vehicle dynamic factor) is to be applied to the spring seats.

The purpose of this test is to evaluate the durability and performance of the axle under varying load conditions. This involves simulating real-world driving scenarios to ensure that the axle can withstand the stresses and strains it will encounter during operation. The actuators used in the test will repeatedly apply the cyclic load, allowing engineers to observe how the axle responds over time. By monitoring the vertical reactions and the behaviour of the spring seats, data will be gathered on the mechanical integrity and lifespan of the axle components. This information is crucial for designing axles that are reliable, safe, and capable of supporting the vehicle's weight under different conditions.

This project has received funding from the European Union's HORIZON EUROPE research and innovation programme under grant agreement No. 101096028. The content of this publication is the sole responsibility of the Consortium partners listed herein and does not necessarily represent the view of the European Commission or its services.

2.1.2 Combined Load

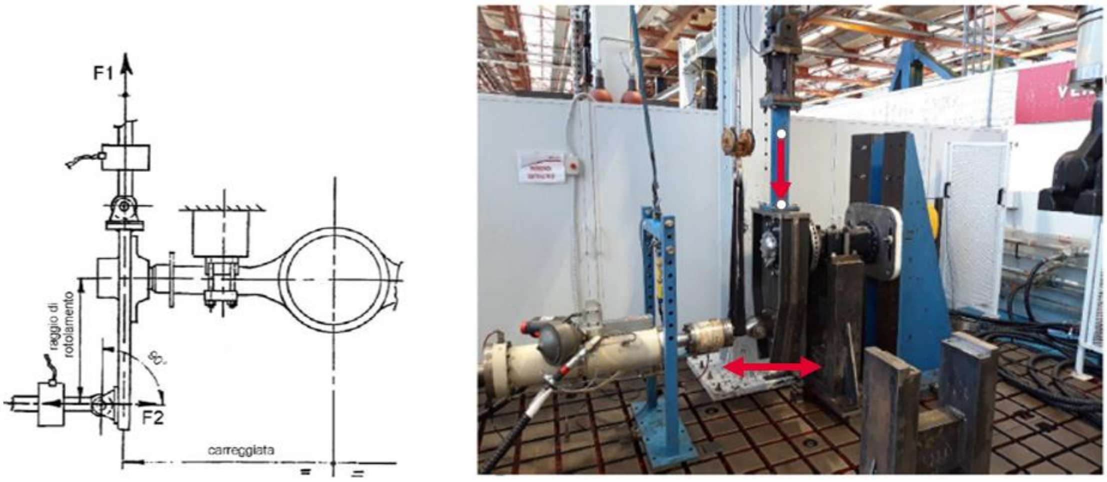

Figure 7: Structural test: combined load.

The axle is constrained using a mechanical setup to allow load application on the wheel end. A vertical static load (F1) and a sinusoidal horizontal force (F2) are applied to the wheel end based on the operating payload of the axle.

A combined load test aims to simulate real-world conditions where axles experience multiple forces simultaneously. This testing method assesses the durability and performance of the axle under various loading scenarios, ensuring it can withstand both vertical and horizontal stresses. By applying these specific loads, engineers can identify potential weaknesses or areas for improvement, ultimately contributing to safer and more reliable vehicle designs.

2.2 Lubrication Test

To ensure performance and durability, the e-axle features integrated oil circuits and electric oil pumps. Lubrication of rotating components is achieved through forced lubrication (using 2 oil pumps) and splash lubrication.

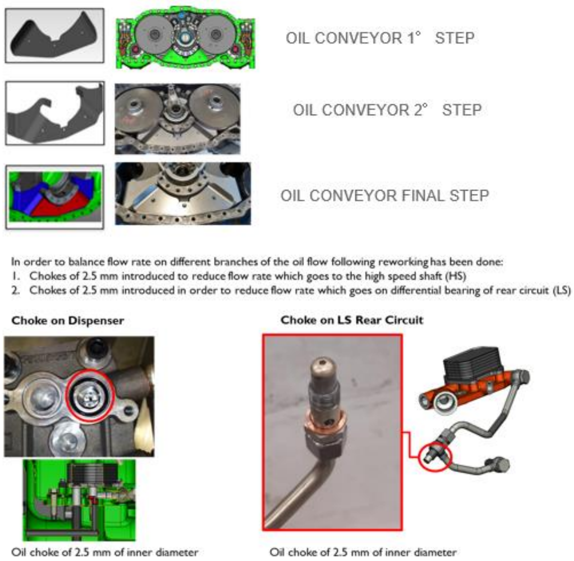

Figure 8: Lubrication test, test bench set-up.

Figure 9: Lubrication test, details.

This project has received funding from the European Union's HORIZON EUROPE research and innovation programme under grant agreement No. 101096028. The content of this publication is the sole responsibility of the Consortium partners listed herein and does not necessarily represent the view of the European Commission or its services.

A lubrication test optimized the design for various speeds, torques, and angles. An e-axle with extra windows and sensors evaluated lubrication, leading to several design changes:

- Splash lubrication: Updated oil conveyor design to protect pump suction elements from turbulent flow, reduce flow speed in the gearbox, and minimize power losses.
- Force Lubrication: Added chokes and nozzles to balance oil flow to bearings, gears, and other components.

These enhancements are part of ongoing efforts to improve the reliability and efficiency of the e-axle system. Engineers also consider the thermal management of the e-axle, integrating cooling systems that prevent overheating and maintain optimal operating temperatures. Continuous monitoring and feedback mechanisms ensure real-time adjustments to the lubrication process, further safeguarding the integrity of the system under varying operating conditions. This holistic approach not only extends the lifespan of the e-axle but also contributes to overall vehicle performance, making it a crucial component in modern automotive engineering.

2.3 Environmental Test

2.3.1 IP69K Certification Test

Figure 10: Overview of dust and water ingress test.

IP (Ingress Protection) testing measures a product's ability to endure high-pressure, high-temperature water jets. IP6K denotes that the device is dust-tight and fully protected against contact. The '9K' indicates the device can withstand high-pressure, steam cleaning procedures.

These tests are essential for ensuring the durability and reliability of devices in challenging environments. For example, products used in industrial or automotive applications often need to meet stringent IP ratings to function effectively and safely under adverse conditions. IP testing helps manufacturers verify that their products can resist dust, water, and other potentially damaging elements. By adhering to these standards, companies can improve the performance and longevity of their devices, thereby enhancing customer satisfaction and reducing maintenance costs.

2.3.2 Environmental Test

Environmental tests confirm the sealing of e-axle across various temperatures and media.

3 Types of Tests Conducted:

- **Thermal cycles**: Cold to warm with high humidity (in air). Thermal cycle testing involves subjecting the e-axle to a series of temperature fluctuations ranging from extremely cold to warm conditions while maintaining high humidity levels. This test aims to simulate the real-world environmental changes that an e-axle might experience during operation. By exposing the e-axle to such rigorous conditions, engineers can assess its durability and performance, ensuring it remains sealed and functional under varying climatic conditions.

This project has received funding from the European Union's HORIZON EUROPE research and innovation programme under grant agreement No. 101096028. The content of this publication is the sole responsibility of the Consortium partners listed herein and does not necessarily represent the view of the European Commission or its services.

- **Water/Ice cycles**: Ambient temperature water, low temperature air. During water/ice cycle testing, the e-axle is exposed to periods of submersion in water at ambient temperature followed by exposure to low-temperature air, simulating freezing conditions. This test helps determine how well the e-axle's sealing holds up against potential water ingress and subsequent freezing, which could cause expansion and potential damage. Successfully passing this test indicates the e-axle's robustness in environments where it may encounter wet and icy conditions.
- **High temperature soak (in air):** The high temperature soak test subjects the e-axle to extended periods in air at elevated temperatures. This test is crucial for evaluating how high temperatures affect the integrity of the e-axle's seals and materials over time. By simulating prolonged exposure to heat, engineers can verify that the e-axle will maintain its performance and sealing properties even in hot climates or during intense operational conditions.

These comprehensive environmental tests ensure that the e-axle is prepared to withstand a variety of harsh conditions, providing reliability and safety for its intended applications. Each test provides valuable data on the performance limits of the e-axle, allowing for improvements and validation of its design and manufacturing processes.

2.4 Durability Test

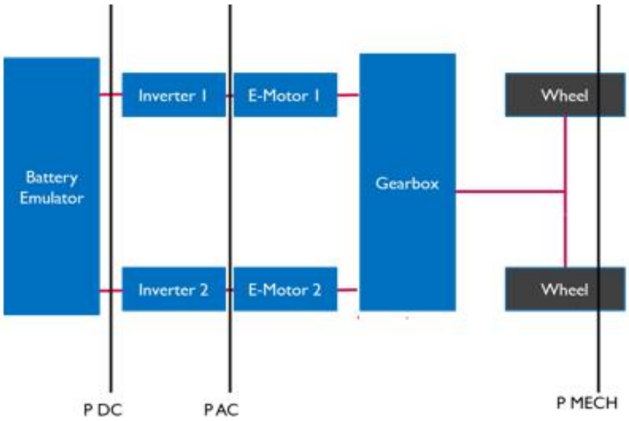

Figure 11: Durability test set-up.

The Durability Test runs e-motors at set speed/torque levels with wheel ends connected to bench brakes to simulate vehicle missions. Its goal is to validate the rotating and electrical parts.

This process involves cycles that mimic real driving conditions, assessing performance and longevity under controlled stress to ensure reliability. These tests improve e-motor design and functionality for safer and more efficient electric vehicles. By reproducing the various stresses and strains that an e-motor will encounter throughout its lifecycle, engineers can identify potential points of failure and work on enhancing durability.

Additionally, the Durability Test includes both thermal and mechanical load variations to closely replicate everyday usage scenarios. These simulations help in understanding how the e-motor behaves under different temperature ranges and power demands, which is critical for optimizing efficiency and preventing overheating or mechanical wear over time. The test also examines how well the motor sustains performance after prolonged exposure to these conditions, ensuring it meets stringent automotive standards.

Another significant aspect of this testing is its role in advancing technology. As electric vehicles become more prevalent, ensuring their components' reliability is paramount. Continuous improvements driven by such rigorous testing not only boost consumer confidence but also contribute to the development of next-generation e-motors that are lighter, more powerful, and environmentally friendly.

This project has received funding from the European Union's HORIZON EUROPE research and innovation programme under grant agreement No. 101096028. The content of this publication is the sole responsibility of the Consortium partners listed herein and does not necessarily represent the view of the European Commission or its services.

The test duration matches the component damage expected by the end of a vehicle's life. This means the e-motor undergoes extensive testing that correlates with years of operational use, providing a thorough evaluation of its resilience. Through these comprehensive evaluations, manufacturers can provide warranties that reflect the actual lifespan of the motor, enhancing trust and satisfaction among customers.

In conclusion, the Durability Test is a crucial phase in the validation of e-motors. It ensures that each component can withstand the demands of daily use while maintaining peak performance. The insights gained from these tests drive innovation and quality in electric vehicle manufacturing, leading to safer, more reliable, and efficient transportation solutions for the future.

2.5 Differential Lock Test

When differential lock is engaged, the wheels are fixed together on the same axle, making them turn at the same speed. This is particularly useful in off-road or slippery conditions where one wheel might lose traction.

Two different tests are executed in order to grant performance and durability of differential lock system. Targets for both static torsion torque as well as durability were reached.

2.5.1 Static Torsional Test

The differential lock is engaged, and the wheel shaft is locked. The differential is rotated to measure the torque and angle at which the system fails. The final torque value needs to be higher than the maximum transmittable torque of the vehicle.

2.5.2 Differential Lock engagement fatigue test

Perform cyclic engagement and disengagement of the differential lock. Ensure that the engagement parameters remain consistent at the beginning and end of the test.

To start, engage the differential lock by activating the control mechanism according to the manufacturer’s instructions. Monitor the system to confirm the engagement has occurred successfully. After a set period, disengage the differential lock and observe the response time and behaviour of the system.

Repeat this cycle several times to verify consistency and reliability. Record any variations in engagement and disengagement times, as well as any anomalies in system performance. It is essential to conduct these tests under controlled conditions to ensure accurate and comparable results. Finally, review the data collected to assess the durability and function of the differential lock over repeated use.

2.6 Gear Shifting test

Specific gear box arrangement used to characterize the shifting system in terms of engagement behaviour under different clutch delta speed identifying the optimal range of delta speed for the activation of the gear shift actuator during the synchronization phase.

Figure 12: Gear Shift Test Set-up.

This project has received funding from the European Union’s HORIZON EUROPE research and innovation programme under grant agreement No. 101096028. The content of this publication is the sole responsibility of the Consortium partners listed herein and does not necessarily represent the view of the European Commission or its services.

Also disengagement test are perfomed in order to identify the max input torque at which actuation system is able to disengage properly.

Full eAXLE system then used to perform full shifting maneuvers which consist of specific events sequence: torque ramp down, gear disengagement, eMotor speed synchronization, requested gear engagement and torque ramp up:

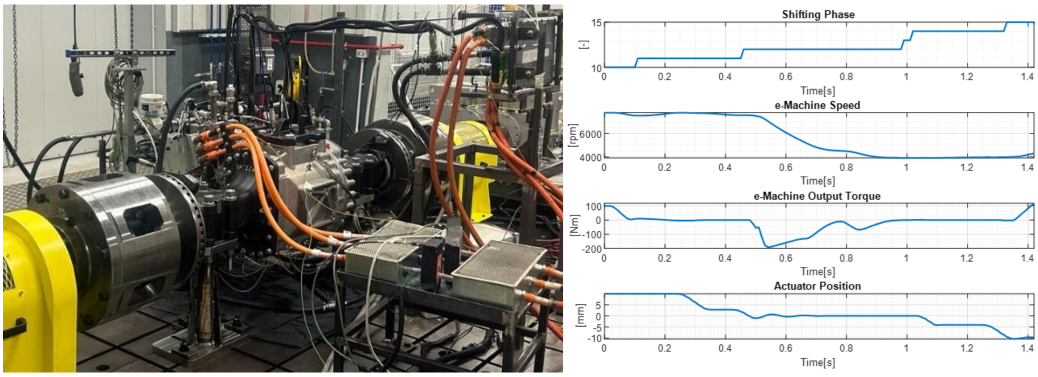

Figure 13: eAxle bench installation and gear shift manoeuvre log.

Test conditions are varied among different torque levels and speeds to verify and calibrate control parameters to optimize shifting manoeuvre in terms of torque-to-torque time, NVH and system stresses

3 First Level Testing and Validation of Fuel Cell System

3.1 Performance Targets Definition

As reported in the D1.1 and D2.2, power and efficiency meeting the performance targets for the FCEV of the EMPOWER project necessitate a thorough understanding of the power demands across different vehicle classes. To this end, a parallel workstream was pursued, focused on identifying the required power output for each application; the numbers anticipated in the preparation of the WP2, were confirmed by the simulation activities, confirming the need to develop a high power and highly efficient system to minimize the H_2 consumption. The H_2 consumption has a double impact: it heavily affects operational costs, and it defines H_2 storage capacity needs for a given mission.

The identified target for fuel cells is towards a 150 kW to 200 kW system, with efficiency above 50 % including low loads that are the least efficient points. This will allow high flexibility and configuration potential:

- 1X system configuration, will allow very good efficiency levels and enough power to cover mountain mission demands, while having a moderate impact on vehicle weight and overall system cost.
- 2X system will allow for outstanding efficiency level, unseen power availability at the expense of increased weight and cost.

This project has received funding from the European Union's HORIZON EUROPE research and innovation programme under grant agreement No. 101096028. The content of this publication is the sole responsibility of the Consortium partners listed herein and does not necessarily represent the view of the European Commission or its services.

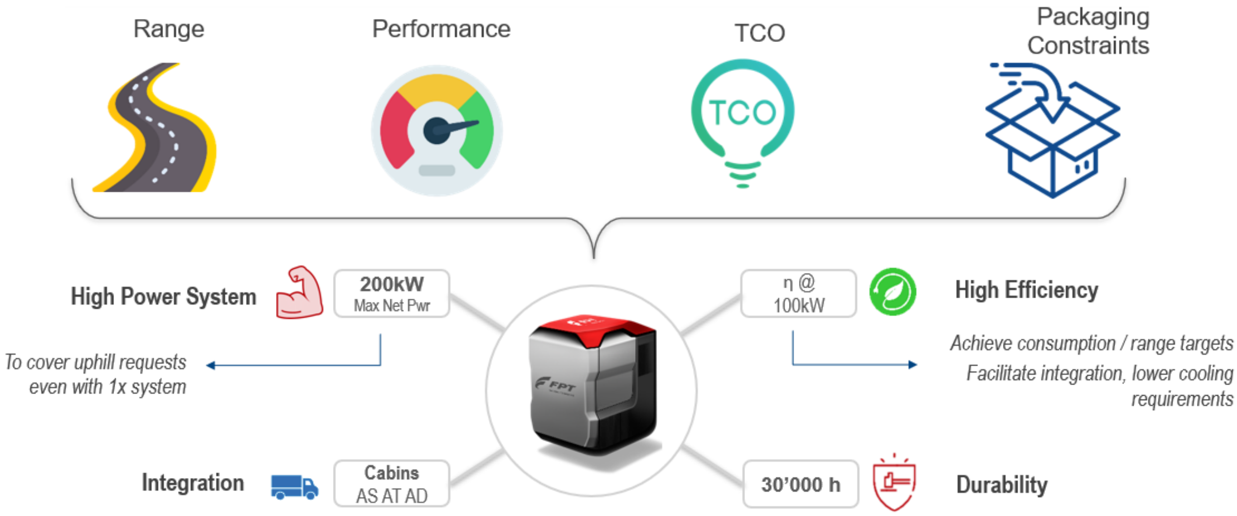

Figure 14: Fuel Cell System main drivers and KPIs summary.

Additionally, the system has been designed with certain targets for the different interfaces that will be subject to be validated during the validation phase:

- **Coolant Interface:** The fuel cell system will have one inlet port and an outlet port for the coolant circuit. The outlet coolant from the fuel cell system will always be below 95 °C.
- **Fuel (H2) Interface:** A stainless-steel Swagelok® connection ensures a H_2 leak tight interface between the fuel cell system and the H_2 supply. The supplied H_2 will be in the range of 16 to 20 bar to ensure the defined system operation.
- **Air Interface:** The fuel cell system is supplied with filtered air in a temperature range between -30 to 40 °C and a relative humidity of 0 to 100 %. A silicon hose with clamp fixation is used as connection to the vehicle air inlet and the vehicle exhaust line. The air filter is installed on the vehicle, not part of the FCS.
- **HV Interface:** The fuel cell system is equipped with standardized HV connectors as an interface to the HV bus. The considered voltage range can vary between 500 to 800 V depending on the battery charging status, which is also to be considered as requirement related to current conversion of the DCDC converter.
- **LV and Communication Interface:** The fuel cell system control unit shall be connected to the vehicle LV battery with a standard connector, and it operates in a range of 18 to 30 V (nominal 24 V). Other LV BoP components of the system will be power supplied via the fuel cell system control unit based on its specifications.
- **Communication Interface – Transmitted signals (FCCU to VCU):** The fuel cell system transmits signals to the vehicle to provide information related to detected faults, operation status as well as the actual fuel cell system net output power.
- **Communication Interface – Received signals (VCU to FCCU):** The fuel cell system receives signals from the vehicle to operate the system in the desired way. The desired operation status and required power are needed during normal run. In case of a crash, the vehicle sends a crash detection signal to trigger the safe system reaction on fuel cell system side.

3.2 Components Testing

Following the detailed description of component selection and design in Deliverable D2.2, comprehensive validation tests and system integration activities were carried out to confirm that each component performed

This project has received funding from the European Union's HORIZON EUROPE research and innovation programme under grant agreement No. 101096028. The content of this publication is the sole responsibility of the Consortium partners listed herein and does not necessarily represent the view of the European Commission or its services.

according to the specified requirements. This section outlines the testing procedures, integration steps, and results for each component of the Cathode and Thermal subsystems.

3.2.1 Cathode Subsystem

The Cathode subsystem is responsible for delivering conditioned air to the fuel cell stack, meeting precise specifications for pressure, temperature, and relative humidity to maintain efficient and stable stack operation. Following component selection and design activities, each component underwent extensive validation testing individually or at subsystem level, and subsequently integrated into the full fuel cell system.

3.2.1.1 Electric Turbocharger

The Electric Turbocharger underwent rigorous validation tests, initially at component level, followed by system-level integration tests. Its performance was measured under controlled operating conditions and compared against simulation predictions obtained through aerodynamic and thermodynamic modelling. Parameters such as air mass flow rate, compression ratio, efficiency, and response time were analysed.

Figure 15 depicts the comparison between simulation results (shown in red) and experimental measurements (shown in green) demonstrates strong alignment. The validation confirmed that the turbocharger consistently met performance targets across the entire operational envelope, reinforcing the accuracy of the initial design simulations and the aerodynamic optimization performed during the design phase.

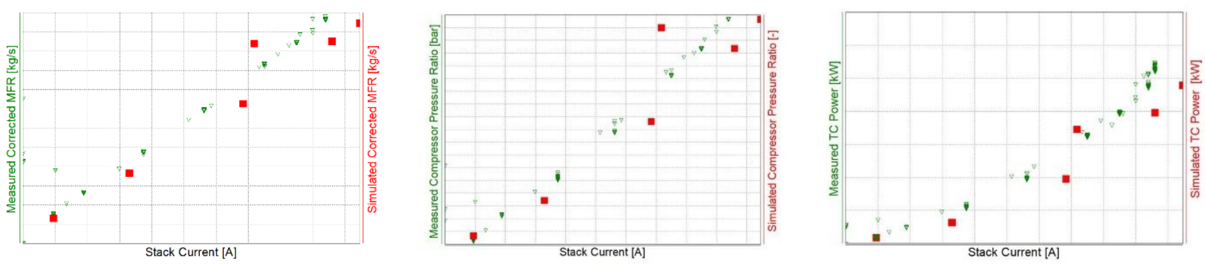

Figure 15: Comparison between simulation (red) and measurements (green) on the Electric Turbocharger.

3.2.2 Humidifier

The Humidifier was thoroughly validated for its humidification performance and pressure-drop characteristics. Tests were conducted to evaluate its performance under varied air flow rates, inlet air humidity conditions, and operating pressures. The experimental results closely matched the manufacturer's provided performance data (Figure 16). This confirmed the suitability of the selected humidifier, demonstrating stable operation and reliable humidification across the fuel cell's operational range.

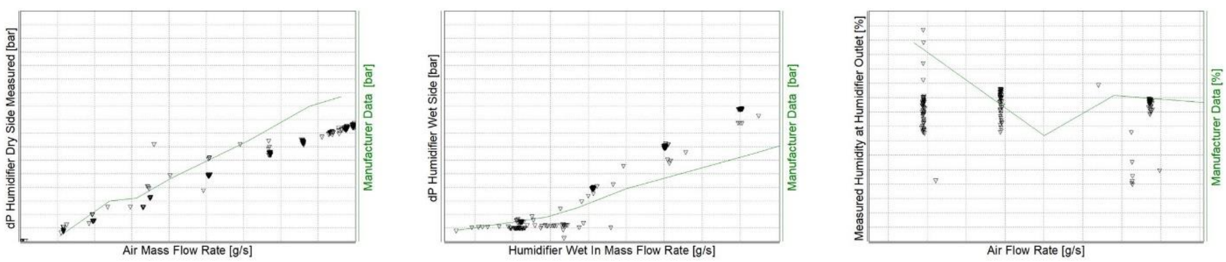

Figure 16: Humidifier: experimental results vs. performance data.

This project has received funding from the European Union's HORIZON EUROPE research and innovation programme under grant agreement No. 101096028. The content of this publication is the sole responsibility of the Consortium partners listed herein and does not necessarily represent the view of the European Commission or its services.

3.2.3 Water Charge Air Cooler

The Water Charge Air Cooler underwent extensive thermal and fluid-dynamic testing. Cooling performance and pressure-drop characteristics were measured under realistic operating scenarios, varying both coolant and air flow rates and temperatures. Results indicated excellent alignment with supplier-provided specifications (Figure 17), confirming that the cooling capability significantly exceeded design requirements. Pressure drops observed on both the coolant and air side matched predictions, demonstrating the component's efficiency and confirming its integration suitability into the cathode air path.

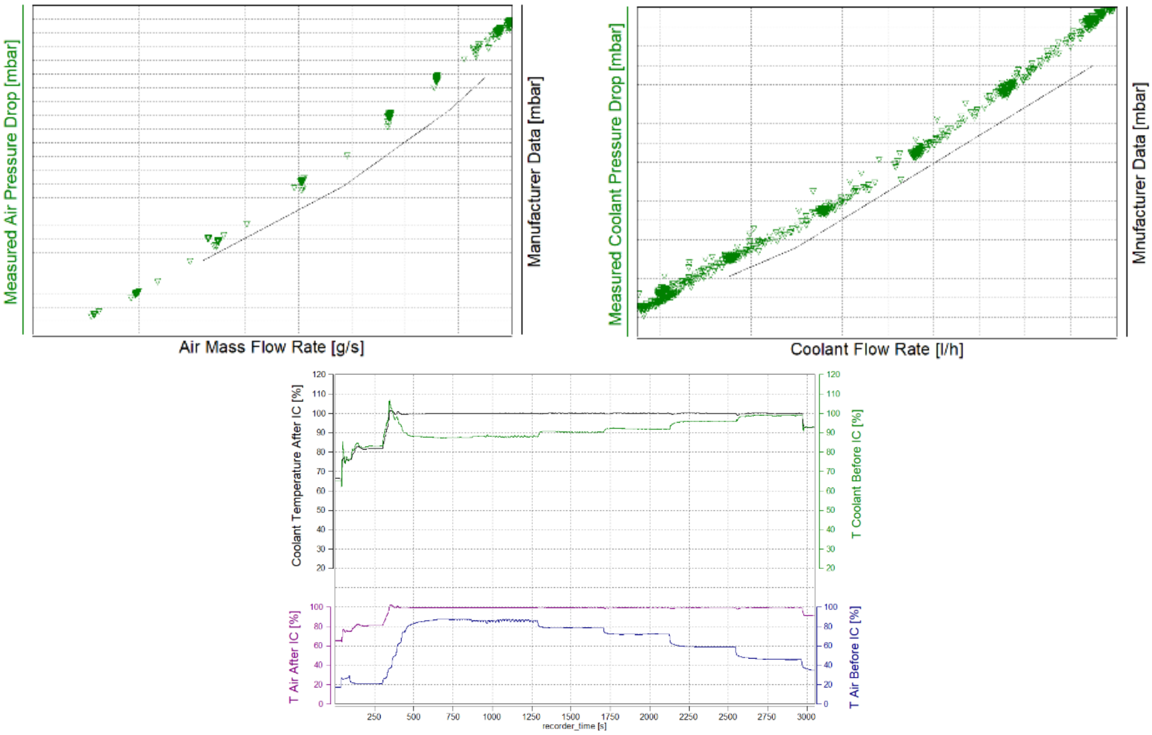

Figure 17: Water Charge Air Cooler: experimental results vs. performance data.

3.2.3.1 Cathode water separator

The Cathode Water Separator is an in-house developed, cyclone-type separator specifically optimized to balance separation efficiency, pressure drop, and compactness. Due to the custom nature of the component, it underwent detailed standalone testing prior to subsystem integration.

A dedicated test bench was built, providing precise control over air velocity, water droplet distribution, and moisture injection rates, thus allowing accurate characterization of separation efficiency and pressure-drop performance. Multiple prototype designs were tested, employing iterative improvements based on the collected experimental data, until the optimum solution was identified.

Final test results demonstrated excellent separation efficiency while maintaining minimal pressure losses, confirming the effectiveness of the optimization efforts. The validated separator was subsequently integrated into the cathode subsystem and further validated in the complete fuel cell system, confirming robust, consistent performance under operational conditions.

This project has received funding from the European Union's HORIZON EUROPE research and innovation programme under grant agreement No. 101096028. The content of this publication is the sole responsibility of the Consortium partners listed herein and does not necessarily represent the view of the European Commission or its services.

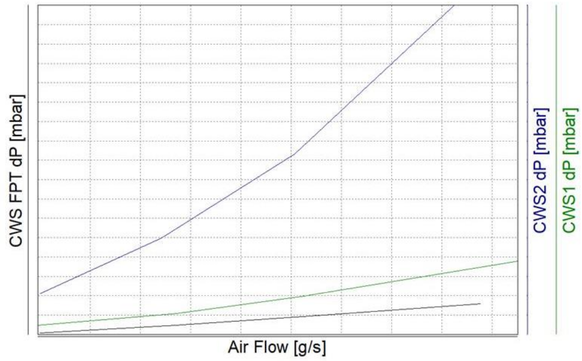

Figure 18: Cathode water separator: comparison of pressure loss at different air flow rates.

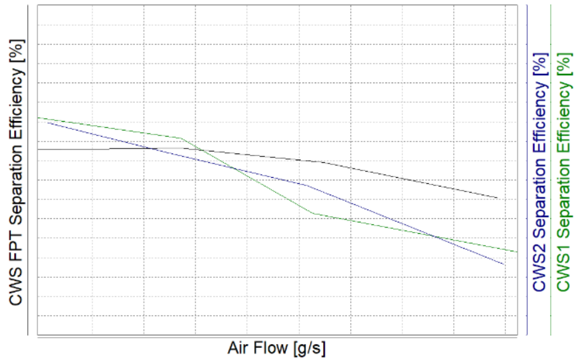

Figure 19: Cathode water separator: comparison of separation efficiency at different air flow rates with a water injection rate of 2g/s.

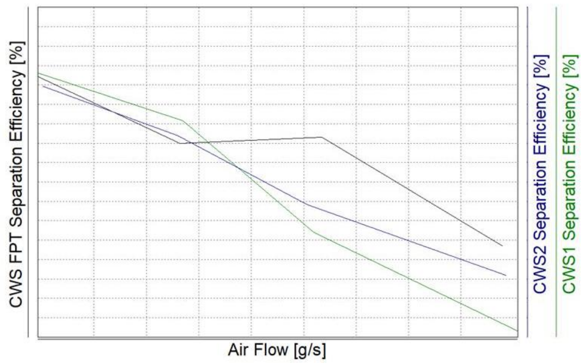

Figure 20: Cathode water separator: comparison of separation efficiency at different air flow rates with a water injection rate of 4g/s.

3.2.4 Thermal Module

As previously detailed in Deliverable D2.2, thermal management in the FPT fuel cell system consists of two distinct coolant loops, each tailored to specific operational needs:

- A High-Temperature (HT) loop, responsible for extracting excess heat generated by the fuel cell stack, and conditioning inlet air through the air-to-water heat exchanger.
- A Low-Temperature (LT) loop, providing temperature control for sensitive high-voltage components (e.g., electric turbocharger, DC-DC converter), which operate optimally at lower coolant temperatures.

Each component of the thermal subsystem underwent targeted testing and validation activities to ensure compliance with design expectations.

This project has received funding from the European Union's HORIZON EUROPE research and innovation programme under grant agreement No. 101096028. The content of this publication is the sole responsibility of the Consortium partners listed herein and does not necessarily represent the view of the European Commission or its services.

3.2.4.1 Pump

The Coolant Pump, a critical element for the reliable and efficient operation of both cooling circuits, was subjected to extensive testing on a dedicated test rig. This specialized facility was equipped with a high-voltage power supply, as well as instrumentation capable of precisely controlling and varying coolant temperatures, flow rates, and system back-pressure.

Validation tests encompassed:

- **Steady-state Performance Mapping:**

  The pump's characteristic curves (flow rate, pressure head, electrical power consumption) were generated at different coolant temperatures, thus recreating the pump's operational map.

- **Transient Performance Evaluation:**

  Dynamic tests were performed to assess pump responsiveness under rapid load changes and varying coolant conditions, mimicking realistic operational scenarios.

Test outcomes confirmed that the pump achieved its specified hydraulic performance targets with consistent reliability and efficiency under both steady-state and transient conditions (Figure 21). This thorough evaluation confirmed the pump's suitability for integration and operation within the fuel cell system's high temperature loop thermal management strategy.

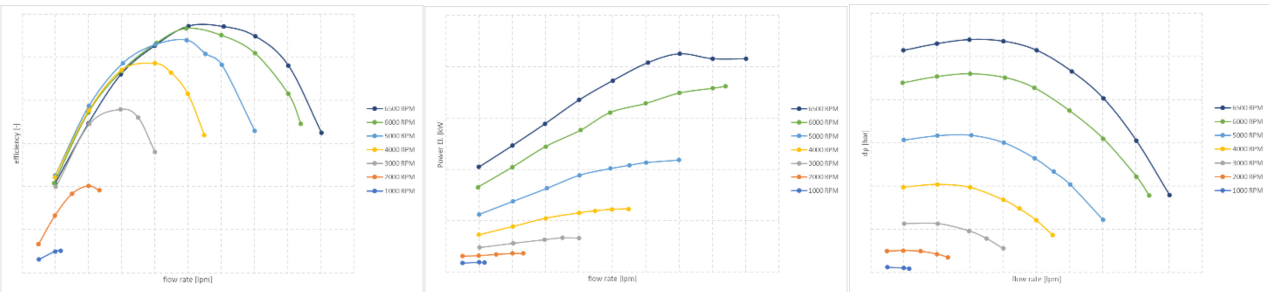

Figure 21: Cooling pump: validation of performance.

3.2.5 Anode subsystem

The anode subsystem is responsible for supplying H2 to the fuel cell stacks at the specified conditions (e.g., pressure, flow rate, H2 concentration) to ensure efficient operation. The design of the passive recirculation concept and the core components required to achieve these targets were described in detail in D2.2. Following component selection and design, extensive validation and integration tests were conducted for each component.

3.2.5.1 Anode Water Separator

The fuel cell system anode water separator is a FPT developed cyclone type separator optimized for the expected water produced at the anode in the stacks by ensuring a high separation efficiency at a low pressure drop (required for the passive recirculation concept).

The anode water separator was tested on a fully customized component test rig where air and water can be supplied under the expected system conditions and measured for different steady-state points. The test was also conducted with two alternative designs available on the market to demonstrate the improved performance.

This project has received funding from the European Union's HORIZON EUROPE research and innovation programme under grant agreement No. 101096028. The content of this publication is the sole responsibility of the Consortium partners listed herein and does not necessarily represent the view of the European Commission or its services.

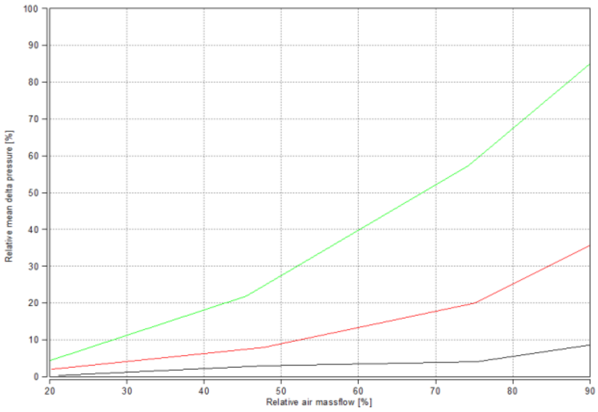

Figure 22: Anode water separator: comparison of pressure drop of the FPT solution (black) and other solutions from the market.

Figure 22 shows that the FPT developed water separator (black) shows better behaviour with respect to relative mean delta pressure in comparison to available solutions on the market (green, red).

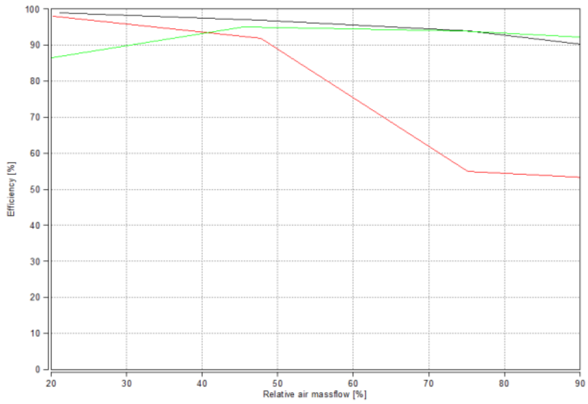

Figure 23: Anode water separator: comparison of efficiency of the FPT solution (black) and other solutions from the market.

Figure 23 shows that the efficiency of the FPT developed water separator (black) slightly decreases over increased relative air mass flow, but still the efficiency shows good results over the whole relative air mass flow range. Other water separators, available on the market, seem to be either optimized for higher air mass flow rates (green) or at lower air mass flow rates (red).

3.2.5.2 Ejector, Injector and Nozzle

The injector is required to supply the stacks with H2 depending on the operation conditions. Choosing a passive recirculation concept also requires a jet pump which consisting of a nozzle and an ejector. All components influence each other; therefore, a customized component test rig is required to validate the performance and conditions of the fuel supply against system requirements.

The maximum H2 mass flow rate is highly dependent on the injector/nozzle combination and the H2 supply pressure, while the recirculation rates depend on the nozzle and ejector. The component test bench enables optimization of the passive recirculation design as described in Figure 24.

This project has received funding from the European Union's HORIZON EUROPE research and innovation programme under grant agreement No. 101096028. The content of this publication is the sole responsibility of the Consortium partners listed herein and does not necessarily represent the view of the European Commission or its services.

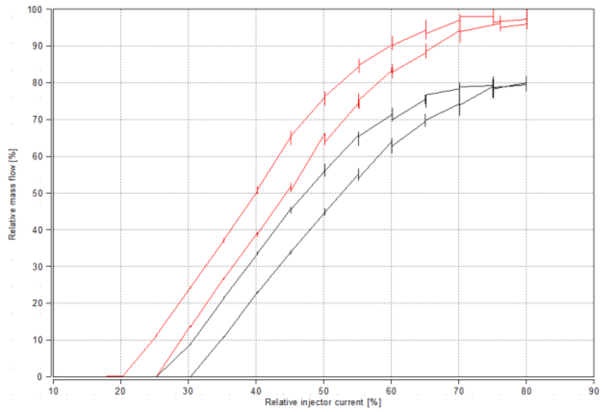

Figure 24: Passive H2 recirculation system: mass flow vs injector current.

Figure 24 shows the mass flow dependency on the H2 supply pressure. The red curve has a 4 bar higher supply pressure than the black one and shows and mass flow increase of around 18 %.

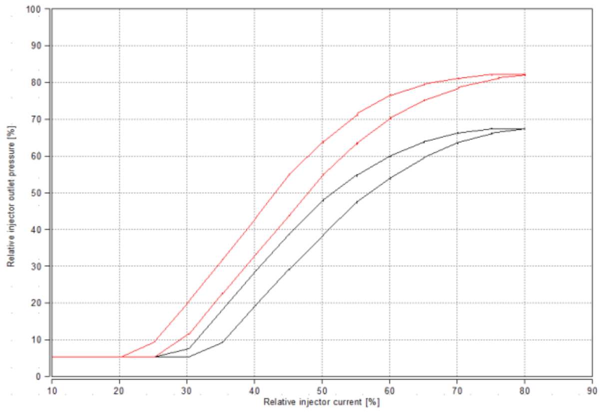

Figure 25: Passive H2 recirculation system: outlet pressure vs injector current.

Figure 25 shows the injector outlet pressure dependency on the H2 supply pressure. The red curve has a 4 bar higher supply pressure than the black one and shows and mass flow increase of around 15 %.

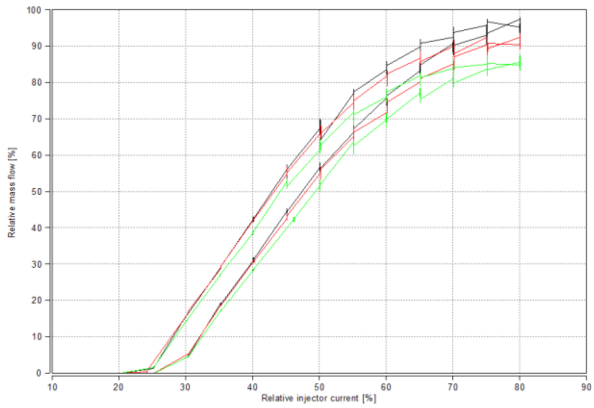

Figure 26: Passive H2 recirculation system: mass flow for different nozzle types.

Figure 26 shows the H2 mass flow dependency on the nozzle type. The black curve shows the result for the nozzle with the largest orifice, whereas the green one has the smallest orifice (advantages in recirculation rates at lower load). The black curve shows a mass flow increase of around 12 % in comparison to the green curve at 80 % injector current.

This project has received funding from the European Union's HORIZON EUROPE research and innovation programme under grant agreement No. 101096028. The content of this publication is the sole responsibility of the Consortium partners listed herein and does not necessarily represent the view of the European Commission or its services.

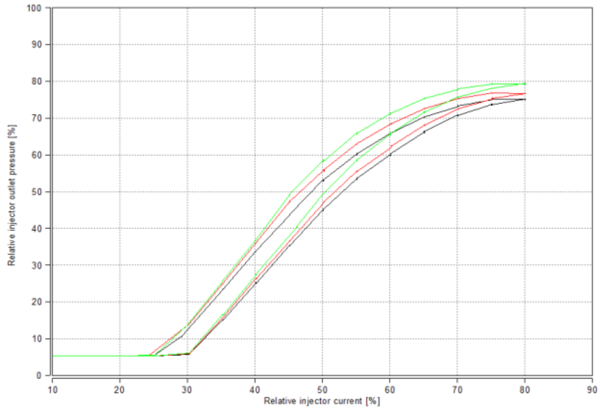

Figure 27: Passive H2 recirculation system: pressure for different nozzle types.

Figure 27 shows the injector outlet pressure dependency on the nozzle type. The green curve shows a slightly higher injector outlet pressure of around 5 % in comparison to the black curve at 80 % injector current, which is due to smaller backpressure effects related to the nozzle orifice.

The concept of passive recirculation is a sufficient concept to operate a fuel cell system with high efficiency, especially under high load conditions. At low load, the performance of the passive recirculation decreases, which is compensated with a pulsating injector control to “trigger” recirculation even below the critical pressure limit between nozzle inlet vs. nozzle outlet.

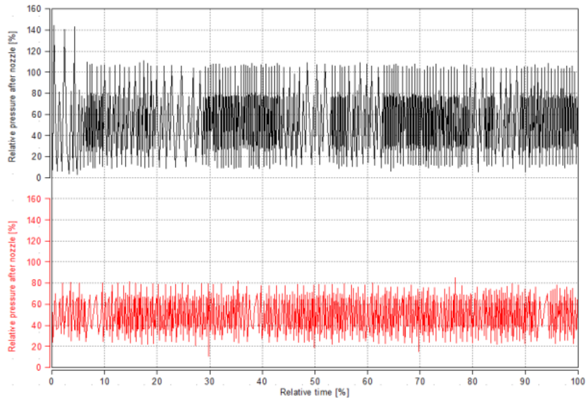

Figure 28: Passive H2 recirculation system: injector pulsation study

Figure 28 shows the frequency dependency of the injector operated in pulsating mode. The black curve (lower frequency) shows an increase of the pressure after the nozzle of about 20 % in comparison to higher frequency. Increased pressure after the nozzle will help to trigger the recirculation even if the critical pressure ratio for supersonic conditions can be not reached.

3.2.5.3 Media Supply Unit

The Media Supply Unit is an in-house developed component required to supply the two stacks with the required medium, meeting the requirements in term of space, material compatibility, flow distribution and external tightness. The design and the material have been tested according to international standards such as ISO 11114 for H2 permeation requirements and ISO12619 for pressurization requirements.

The following pressure profile was designed based on ISO 12619 and executed with helium as test gas. The leakage rate was calculated considering all the components installed at the Media Supply Unit and measured over the whole test duration. A helium sniffer was used to detect external leaks during the test.

This project has received funding from the European Union’s HORIZON EUROPE research and innovation programme under grant agreement No. 101096028. The content of this publication is the sole responsibility of the Consortium partners listed herein and does not necessarily represent the view of the European Commission or its services.

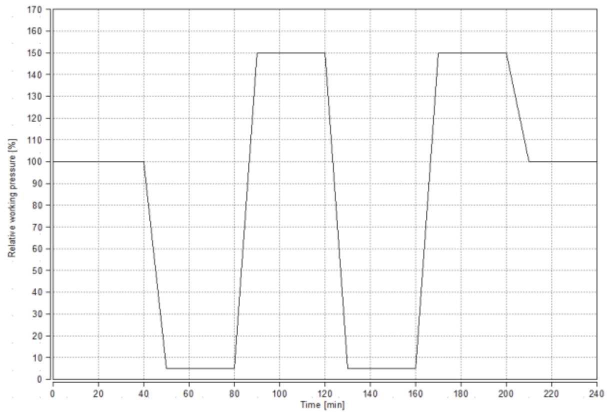

Figure 29: Media Supply Unit: pressure profile for stress test.

Figure 29 shows the predefined pressure profile to perform the Media Supply Unit stress test to verify that the material and design can withstand the mechanical stress while ensuring the leakage targets based on ISO 12619. The leakage rate was meeting the requirements from ISO 12619 and no deformation was observed.

Furthermore, a hydrostatic strength test was executed, where the component was pressurized up to ten times of the expected working pressure without any visible rupture. Another leakage test was performed afterwards to ensure that the external tightness was maintained.

To validate that the flow is distributed equally to the two stacks a CFD simulation was executed to optimize the design accordingly.

3.3 FC system testing - Description of Test Procedures

The testing campaign performed on a FC system aims at providing important information and answering fundamental questions that regard the product and to understand its capabilities and limitations. The programmed tests target to give answers to the following questions:

- Does the product deliver according to its specification?
- What are its limitations, e.g. on the maximum power, power slope, temperature, and humidity conditions etc?
- What is its dynamic behaviour?
- What is the time from startup to maximum power?
- What is its efficiency across its performance span?
- How is it degrading?
- Finally, can it be used for the planned missions?

To obtain comprehensive answers to the above questions FMF has designed a series of tests that cover different aspects of the product's behaviour and performance. The tests are divided into two main groups, the technical cycles, and the missions.

3.3.1 Technical cycles

The technical cycles are generic tests performed on the FC system test bench that do not correspond to real operating conditions, rather they illuminate specific characteristics of the product's behaviour. The cycles used here are the following:

This project has received funding from the European Union's HORIZON EUROPE research and innovation programme under grant agreement No. 101096028. The content of this publication is the sole responsibility of the Consortium partners listed herein and does not necessarily represent the view of the European Commission or its services.

Downward Polarisation Curve (POL)

This is the typical polarization curve performed in most fuel cell cases and used to characterise their steady-state behaviour. In this project the process is restricted to the downward part, i.e.:

- Preheating (if no other test has preceded)
- Ramping up in short steps to the maximum
- Stepping down from maximum in pre-defined steps and time intervals. On each step the data used for the steady-state calculation corresponds to the time from –130 s up to –10 s before the end of the step, which is a 120 s time span with a 10 s offset.

Dynamic Polarisation Curve (DPOL)

Contrary to the typical polarisation curve the DPOL is giving a first view of the FC's dynamic behaviour, especially its over- and undershoot in a systematic way. This cycle is essentially sweeping the power between minimum (idle) to maximum with variable power change rates (±0.5 kW/s, ±1 kW/s, ±2 kW/s, ±4 kW/s, ±8 kW/s, ±16 kW/s, ±32 kW/s, ±40 kW/s and ±50 kW/s).

Step Test (STST)

STST is a load cycle used to evaluate system response under progressive power demand conditions. The test consists of incrementally increasing the power output of the fuel cell system in fixed steps of 20 kW, starting from the minimum operating point and continuing up to the maximum rated power. Each step is maintained for a duration of 45 minutes to ensure that the system reaches thermal and operational equilibrium at each load level. This procedure enables the detailed assessment of system behaviour, particularly in relation to thermal management, component stability, and overall performance consistency under stable load conditions.

3.3.2 Missions

The missions' testing helps acquiring a more practical and application-oriented understanding of the FC system's performance. The tested missions stem from real vehicle missions that have been considered as reference during the simulation phase of the EMPOWER project considering the selected components and hybridization strategy. From those simulations the FC power demand is extracted and used as power demand input on the test bench. Often, such missions are extracted once for specific FC truck configurations and then adapted to the boundary conditions of the UUT. This is the case for this testing campaign as well.

In this project, four missions are used. For confidentiality reasons, details of the missions are not divulged here. The used missions are the following:

- Long-haul ACEA mission (ACEA) → 1 & 2 systems configuration
- Heavy-duty mountainous 1 (BR) → 150 kW (2 systems)

3.3.3 Ambient Condition Validation Testing

To further validate the robustness and reliability of the fuel cell system under extreme environmental conditions, targeted ambient tests are planned using an external conditioning unit capable of supplying air flows up to 660 kg/h with precise control of temperature (up to 35 °C) and relative humidity (up to 80% RH). The validation protocol will encompass a series of steady-state cycles, including controlled temperature sweeps and humidity sweeps at fixed loads. Additionally, downward-only polarization curves will be conducted at predefined combinations of high temperature and humidity conditions. These tests are designed to rigorously assess system performance, durability, and operational stability under challenging real-world scenarios.

This project has received funding from the European Union's HORIZON EUROPE research and innovation programme under grant agreement No. 101096028. The content of this publication is the sole responsibility of the Consortium partners listed herein and does not necessarily represent the view of the European Commission or its services.

3.4 Monitoring function validation

As discussed in Deliverable 2.2, the monitoring and diagnosis function is crucial for automotive systems to ensure the safety of both occupants and the vehicle or powertrain from potential hazards. This function continuously monitors fuel cell system components (such as sensors and actuators) and system parameters for any malfunctions or anomalies. Fault levels are categorized into five different levels, represented by the signal FCCU_stFltLvl, as shown in Table 4. To validate the monitoring and diagnosis function, several examples have been demonstrated.

Table 4: Fault level

Fault Level	Status
None	0
Warning	1
Soft-derate	2
Hard-derate	3
Limp home	4
Shutdown	5
Fatal	6

Demonstration of Soft derate function:

The Soft derate functions have been demonstrated in this example on high delta temperature between stack inlet and outlet as shown in Figure 30. The threshold is set at 74% for 20 sec. In case the delta temperature is exceeded this threshold for the predefined debounce time a power Soft derate function will be triggered, as presented in the below figure. Once the fault is detected, the desired power demand is ignored, and the system operating power is reduced until the delta temperature reduced below the threshold. Once the delta temperature is reduced below the threshold then the current increases to follow the current demand.

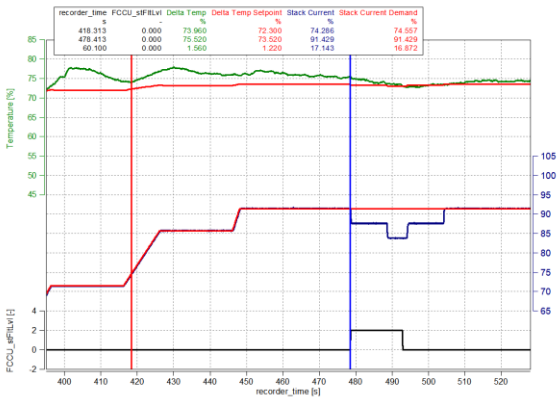

Figure 30: Soft derate request demonstration due to high stack coolant delta temperature.

Demonstration of Fault Shutdown function:

In absence of CAN communication between the CVM and FCCU, shutdown is triggered by the FCCU to avoid system operation without the CVM measurements as shown in Figure 31. The debounce time for this fault confirmation is set to 2sec. the FCCU trigger a shutdown to avoid running the system without certain cell voltage measurement. The debounce time of this failure is set to 2 sec. That applies to all actuators which are using CAN communication, such as turbocharger, coolant pump, etc.

This project has received funding from the European Union's HORIZON EUROPE research and innovation programme under grant agreement No. 101096028. The content of this publication is the sole responsibility of the Consortium partners listed herein and does not necessarily represent the view of the European Commission or its services.

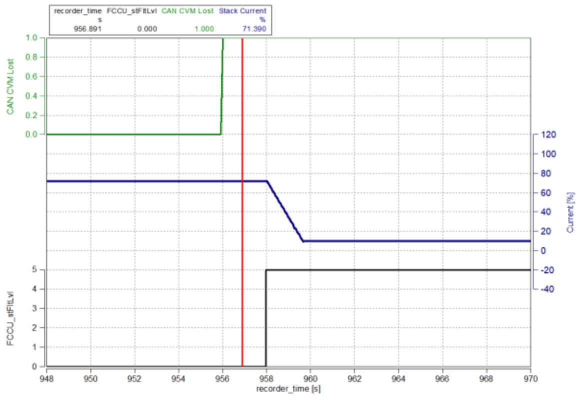

Figure 31: Shutdown request demonstration due to loss of CAN communication.

Demonstration of Emergency Shutdown function:

In absence of high voltage to the turbocharger or the coolant pump, an emergency shutdown request is triggered in order to protect the system as shown in Figure 32. The debounce time for this fault confirmation is set to 0.03sec.

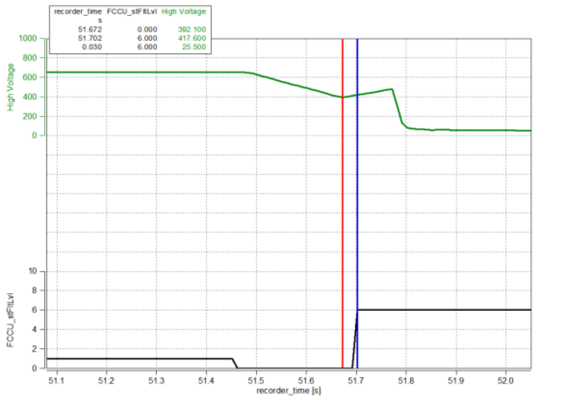

Figure 32: Emergency Shutdown request demonstration due to loss of high voltage.

Demonstration of Fault Shutdown function:

A protection of delta temperature between stack inlet and outlet is implemented. The threshold is set at 80% for 5 sec. In case the delta temperature is exceeded this threshold for the predefined debounce time a Shutdown request will be triggered as shown in Figure 33.

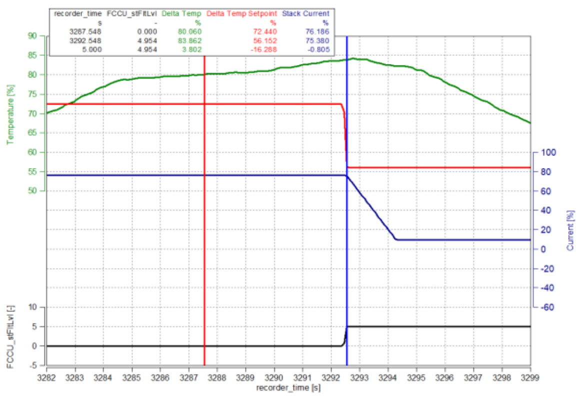

Figure 33: Shutdown request demonstration due to high coolant delta temperature.

This project has received funding from the European Union's HORIZON EUROPE research and innovation programme under grant agreement No. 101096028. The content of this publication is the sole responsibility of the Consortium partners listed herein and does not necessarily represent the view of the European Commission or its services.

Demonstration of Soft derate function:

In case of the coolant pump overheating monitoring is detected, a soft-derate function is triggered by the FCCU within 60secs to avoid pump emergency failure. The desired power demand is ignored, and the system operating power is reduced until the pump overheating signal is recovered as shown in Figure 34.

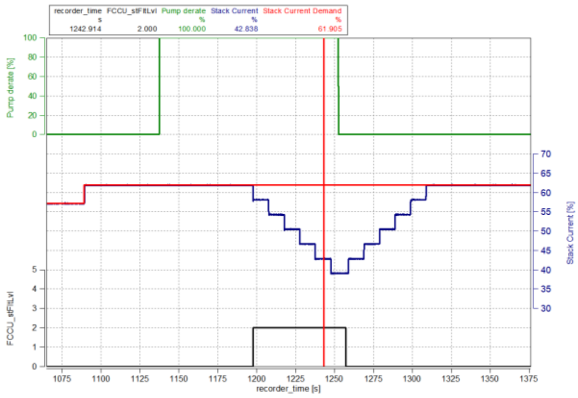

Figure 34: Soft derate request demonstration due to coolant overheating fault detection.

3.5 Performance assessment under load step variation

The control performance assessment is mainly validated at constant stack current over defined operating conditions (i.e. flow, pressure, temperature etc.) for each subsystem. The operating condition depends on the stack load current and is defined by the stack supplier that optimize stack performance and lifetime. The subsystem controller was implemented to achieve the operating conditions given by the stack supplier at given load current. The subsystem control description and steady-state performance are as follows.

3.5.1 Air subsystem Control

The airpath controller requirements are to regulate the cathode stack mass flow and stack inlet pressure given by the stack supplier at given stack current. The control inputs used to achieve the desired operating conditions are the turbocharger speed and back-pressure valve position. A feedforward + feedback close loop control architecture is used to derive control inputs (turbocharger speed and back-pressure valve position) to achieve the above desired operating conditions. The control architecture performs satisfactory under system model uncertainty and unknown disturbances with minimal oscillations. The air flow controller regulates the stack flow by changing the turbocharger speed.

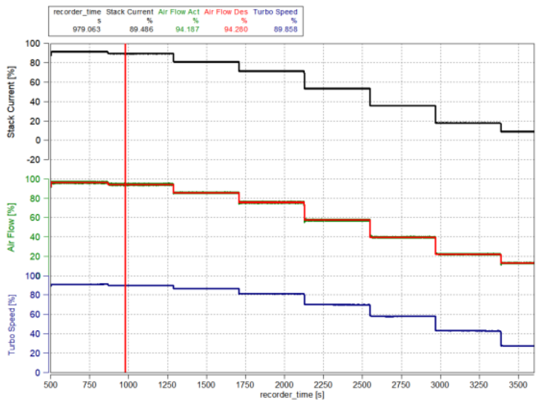

Figure 35: Cathode stack inlet flow control response and back pressure valve opening.

This project has received funding from the European Union's HORIZON EUROPE research and innovation programme under grant agreement No. 101096028. The content of this publication is the sole responsibility of the Consortium partners listed herein and does not necessarily represent the view of the European Commission or its services.

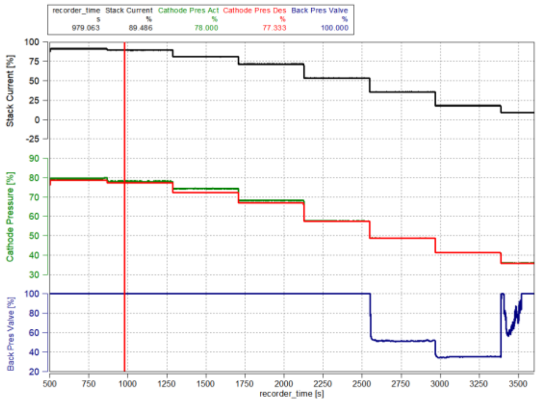

Figure 36: Cathode stack inlet pressure control response and back pressure valve opening.

The controller meets the steady-state stack flow requirements as shown in Figure 35. The air pressure controller regulates the stack inlet pressure by changing the back-pressure valve position. The steady-state stack inlet pressure is not completely achieved specially at higher load points due to high system back-pressure as a result the back pressure valve is fully opened as shown in Figure 36.

3.5.2 Anode subsystem Control

The anode controller requirement is to regulate the anode stack inlet pressure (given by the stack supplier) under pressure disturbance from purge and drain events at given stack current. A feedforward and PI based close loop feedback controller architecture is used to derive control input injector duty-cycle to achieve desired anode stack inlet pressure. The controller meets the steady-state anode stack inlet pressure requirements as shown in Figure 37.

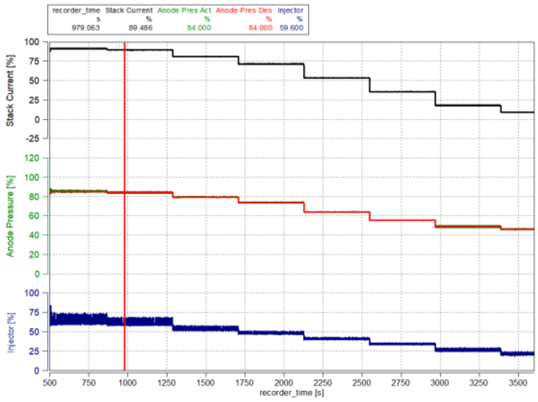

Figure 37: Hydrogen stack inlet pressure and the injector duty cycle.

3.5.3 Thermal subsystem Control

The thermal controller requirements are to regulate the coolant stack delta-temperature (i.e. difference between stack outlet and stack inlet temperature) and coolant stack inlet temperature given by the stack supplier at given stack current. The control inputs used to achieve the above desired operating conditions are the coolant pump speed and three-way valve position. A feedforward and PI based close loop feedback controller architecture is used to derive above control inputs to achieve desired operating conditions. The coolant stack delta-temperature controller regulates the stack delta-temperature by actuating the coolant pump speed. The controller meets the steady-state stack delta-temperature requirements as shown in Figure 38. The coolant stack inlet temperature controller regulates the stack inlet temperature by actuating the three-way valve position. The controller meets the steady-state stack inlet temperature requirements as shown in Figure 39.

This project has received funding from the European Union's HORIZON EUROPE research and innovation programme under grant agreement No. 101096028. The content of this publication is the sole responsibility of the Consortium partners listed herein and does not necessarily represent the view of the European Commission or its services.

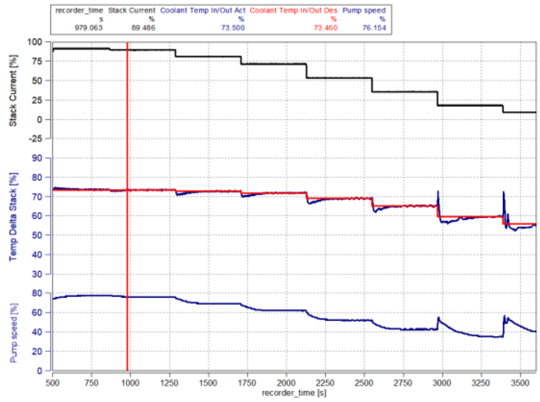

Figure 38: Coolant delta temperature response and coolant pump speed.

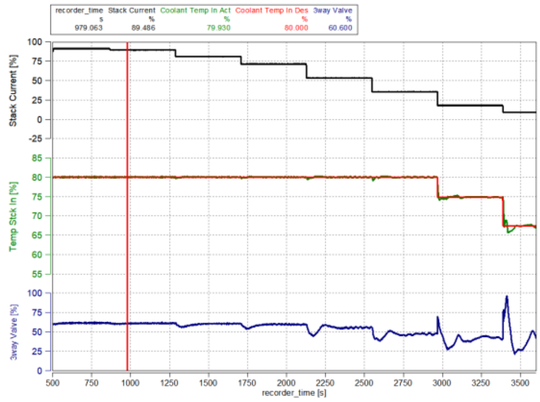

Figure 39: Coolant stack inlet temperature and three-way valve position.

3.5.4 System net power

The system net power output depends on DCDC output power (stack power generation and DCDC conversion), turbocharger power consumption and low voltage consumption whereas the hydrogen input power is calculated based on the Lower Heating Value (LHV) of hydrogen and hydrogen mass flow taking part in the electrochemical reaction. The net system power calculation is given as follow:

$$P_{net} = P_{DCDC} - P_{Cmpr} - P_{LV}$$

where P_{net} = System net power output (kW)

P_{DCDC} = DCDC power output (kW)

P_{Cmpr} = Compressor power consumption (kW)

P_{LV} = LV power consumption (kW)

$$P_{H2} = LHV_{H2}.\dot{m}_{H2,reac}$$

where P_{H2} = System H2 power input (kW)

LHV_{H2} = Lower Heating Value of H2 (MJ/kg)

$\dot{m}_{H2,reac}$ = reacting H2 mass flow rate (g/s)

This project has received funding from the European Union's HORIZON EUROPE research and innovation programme under grant agreement No. 101096028. The content of this publication is the sole responsibility of the Consortium partners listed herein and does not necessarily represent the view of the European Commission or its services.

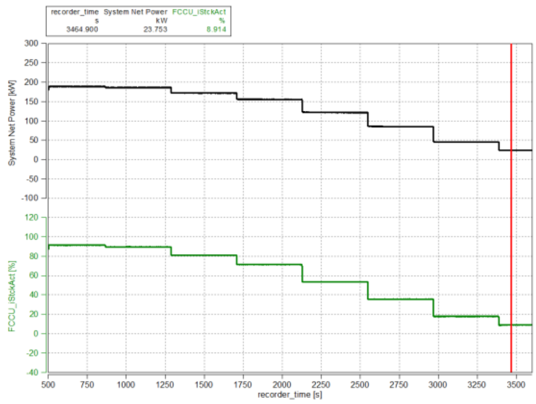

Figure 40: System net power.

3.6 Performance Assessment

Unlike the previous section, when the electric vehicle is under driving cycle, a faster power demand can be requested. For that system validation under technical cycles and missions is a must in order to prove its robustness and response time.

3.6.1 Dynamic Polarisation Curve

Figure 40 illustrates the outcome of a Dynamic Polarisation Curve (DPOL) test, where the fuel cell system is subjected to a series of rapid load transitions with varying ramp rates. The black line represents the load request as defined by the test cycle, while the green line shows the actual load delivered by the system over time.

The purpose of this test is to evaluate the system's dynamic behaviour, particularly its ability to follow abrupt changes in power demand without significant performance deviations. The observed results indicate that the fuel cell system exhibits a strong dynamic response. While minor overshoots are visible following the sharp load increases, they remain well within acceptable limits and are quickly corrected. The actual load consistently stabilizes to match the requested value in a short timeframe, demonstrating effective control logic and responsive BoP coordination.

Overall, the system performance in this DPOL test is judged to be robust. The controlled nature of the overshoot and the rapid return to steady-state values confirm the system's capability to handle dynamic power demands reliably, making it suitable for real-world applications that involve frequent and rapid load changes, such as heavy-duty vehicle operation.

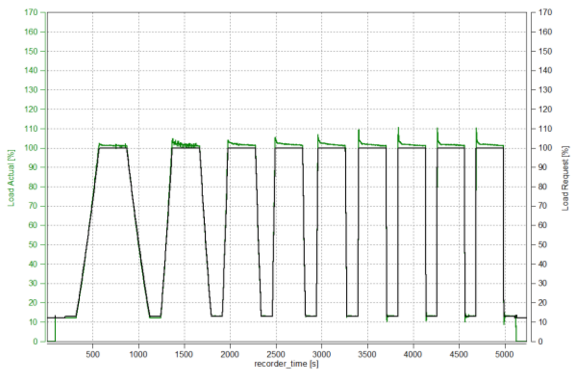

Figure 41: Dynamic Polarization Curve Results.

This project has received funding from the European Union's HORIZON EUROPE research and innovation programme under grant agreement No. 101096028. The content of this publication is the sole responsibility of the Consortium partners listed herein and does not necessarily represent the view of the European Commission or its services.

3.6.2 ACEA Long Haul Mission

In this section, the Gen1 FPT fuel cell system has been tested under ACEA driving cycle, where the power varies between 24kW to 150kW for 1.3 hours. The overall results show that the controllers are robust against fast increase and decrease of power demand.

In Figure 42, the actual net power (blue line) is compared with the power demand (red line). It can be seen that the power controller is able to follow its desired.

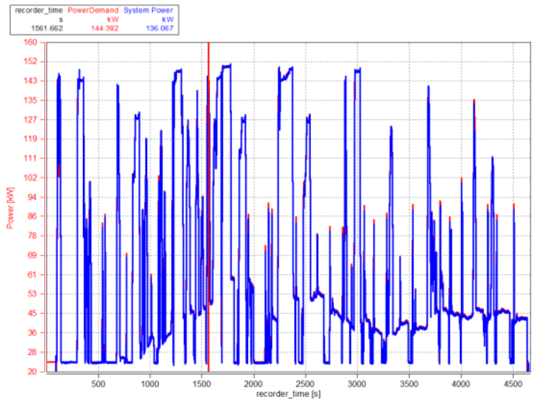

Figure 42: ACEA driving cycle mission.

Figure 43 illustrates the air flow control performance under a driving cycle with its controller turbocharger speed.

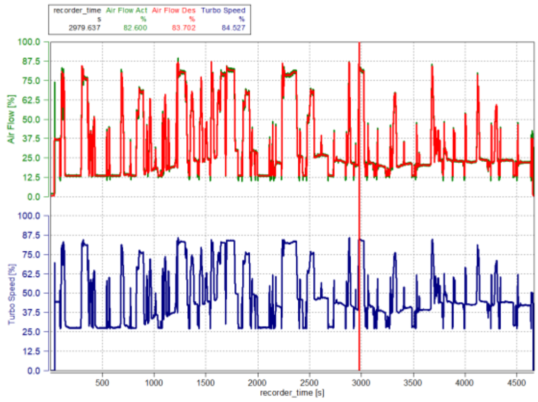

Figure 43: Air flow control response during driving cycle.

Figure 44 illustrates the cathode inlet pressure and the back pressure valve position. It can be seen that the actual cathode stack inlet pressure (green line) is following its setpoint (red line) during transient. It can be noticed that the cathode pressure is slightly higher due higher system back pressure, a point to be improved with future iteration. For that, it can be seen that the back pressure valve is fully open while the actual pressure is slightly higher than its setpoint.

This project has received funding from the European Union's HORIZON EUROPE research and innovation programme under grant agreement No. 101096028. The content of this publication is the sole responsibility of the Consortium partners listed herein and does not necessarily represent the view of the European Commission or its services.

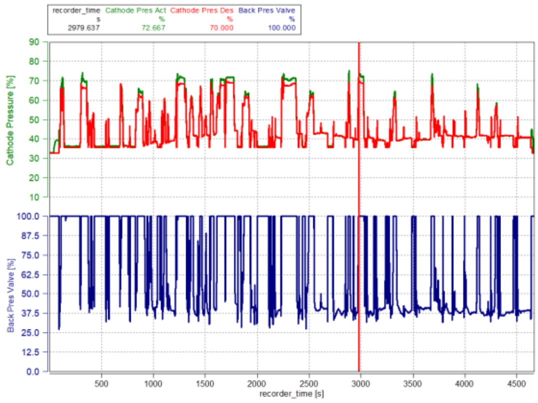

Figure 44: Air pressure response during driving cycle.

Figure 45 illustrates the anode stack inlet pressure, and it is controller variable the Injector valve duty cycle. It can be seen that the anode pressure (green line) follows its setpoint (red line) despite the high power demand variation.

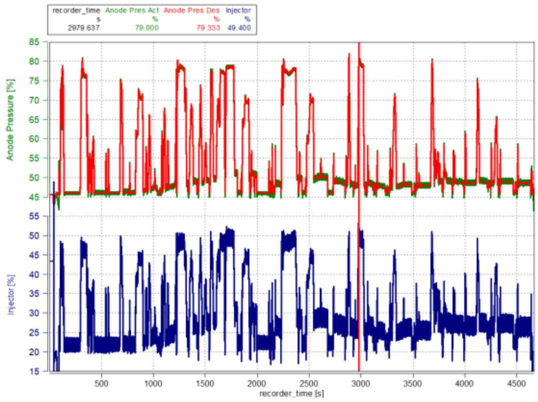

Figure 45: Hydrogen pressure response during driving cycle.

Figure 46 illustrates the coolant stack inlet temperature and its control variable the three-way valve. It can be seen that the temperature is following its setpoint despite short overshoot and undershoot.

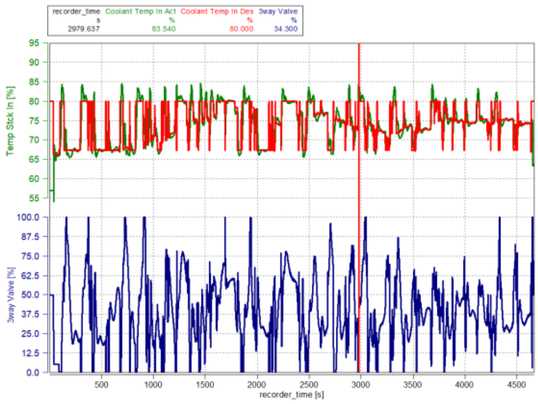

Figure 46: Coolant stack inlet temperature response during driving cycle.

Figure 47 illustrates the delta coolant temperature, i.e. different between coolant stack outlet temperature and coolant stack inlet temperature, and it is control variable which is the coolant pump speed. It can be seen that the delta temperature is following its setpoint. However short overshoot and undershoot are identified.

This project has received funding from the European Union's HORIZON EUROPE research and innovation programme under grant agreement No. 101096028. The content of this publication is the sole responsibility of the Consortium partners listed herein and does not necessarily represent the view of the European Commission or its services.

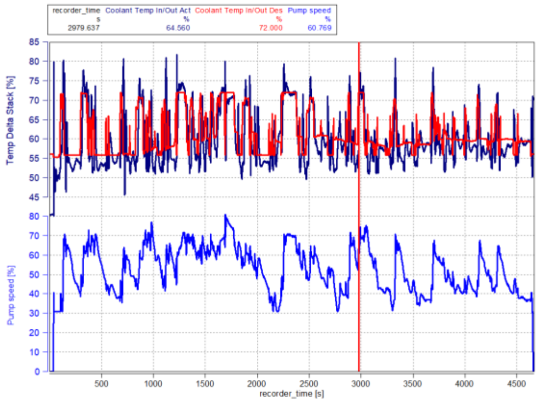

Figure 47: Coolant delta temperature response during driving cycle.

Additional driving cycle mission has been tested in order to validate the robustness under several conditions. For example, Brenner driving cycle is applied where the power varies between 24 kW to 150 kW for 3.7 hours. The power response is presented in Figure 48 with a zoom on a short time window in Figure 49.

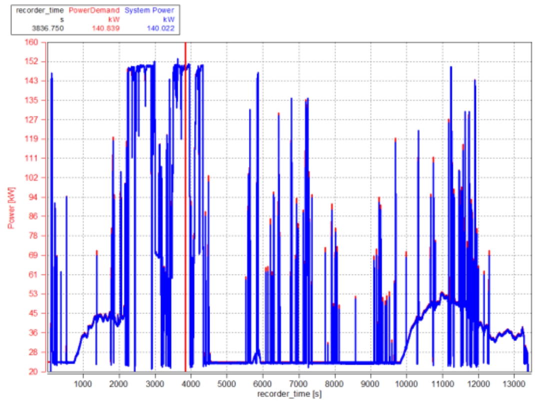

Figure 48: Power driving cycle response under Brenner mission.

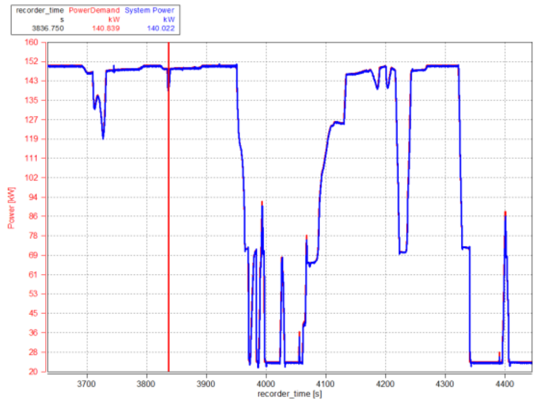

Figure 49: Short window power driving cycle response under Brenner mission.

3.6.3 Ambient Condition Testing

This test series presents the outcome of several downward polarisation curves conducted under controlled high-temperature and high-humidity ambient conditions. The test was executed using an air conditioning unit set to maintain a constant inlet air temperature of 35 °C and relative humidity (RH) levels of 20%, 40%, 60%, and 80%, respectively. The aim was to assess the fuel cell system's performance and resilience when

This project has received funding from the European Union's HORIZON EUROPE research and innovation programme under grant agreement No. 101096028. The content of this publication is the sole responsibility of the Consortium partners listed herein and does not necessarily represent the view of the European Commission or its services.

subjected to elevated ambient conditions, specifically evaluating air handling, humidification effectiveness, and thermal management across the air path.

Figure 49 confirms the execution of a downward polarisation protocol, with power output reduced stepwise over the course of the test. This consistent load profile provides a stable baseline for evaluating how the system handles thermal and humidity variations.

The air temperature measured at the compressor outlet (Figure 52) shows clear stepwise behaviour, mirroring the load curve. This temperature progressively decreases as power is reduced, consistent with expected compressor and flow dynamics. Despite the elevated inlet temperature setting of the conditioning unit, the temperature at the stack inlet (Figure 53) remains within a tightly controlled range and consistently below or near the normalised nominal value. This result demonstrates effective thermal regulation by the BoP components, confirming that the system is capable of maintaining proper stack inlet temperature even under elevated ambient air temperatures.

In terms of humidity, the compressor inlet air humidity (Figure 51) shows visible oscillations, which are attributed to the dynamic control behaviour of the conditioning unit. These oscillations are also evident in the corresponding compressor inlet air temperature plot (Figure 50), further supporting the diagnosis of fluctuating input conditions. Nevertheless, the air humidity at the stack inlet (Figure 54) remains relatively well-controlled, with each curve following a distinct and consistent trajectory that correlates with the respective RH setpoints. While minor fluctuations are observed, they remain within acceptable bounds and do not appear to compromise stack operation.

Overall, the results confirm that the fuel cell system exhibits stable performance across a wide humidity range even when operated with high inlet air temperature. The temperature control strategy proves effective, maintaining stack inlet conditions within the desired range. Similarly, the humidification strategy is able to preserve appropriate moisture levels at the stack inlet, despite external disturbances introduced by the conditioning unit. These findings support the robustness of the system's air and thermal management subsystems and validate the viability of operation in demanding environmental conditions.

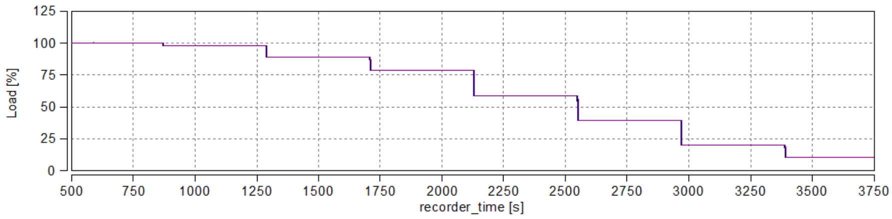

Figure 50: Downward Polarization Curve Load Steps.

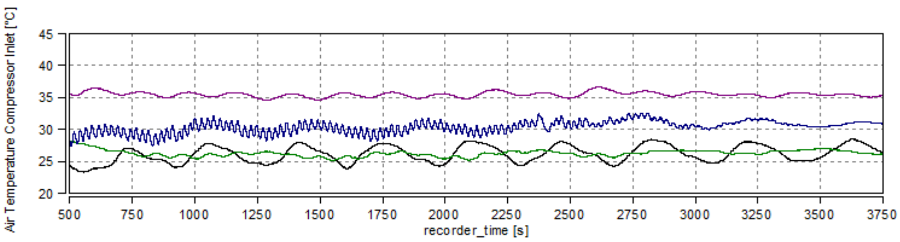

Figure 51: Air Temperature at Compressor Inlet.

This project has received funding from the European Union’s HORIZON EUROPE research and innovation programme under grant agreement No. 101096028. The content of this publication is the sole responsibility of the Consortium partners listed herein and does not necessarily represent the view of the European Commission or its services.

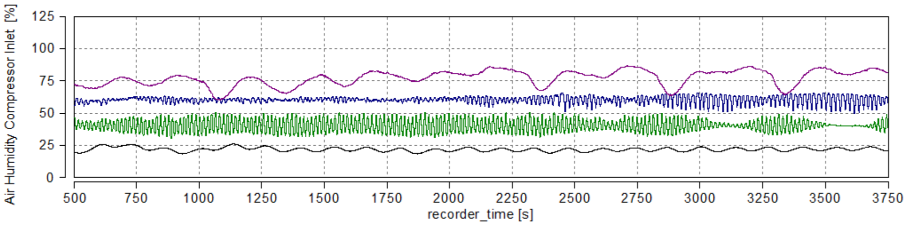

Figure 52: Air Humidity at Compressor Inlet.

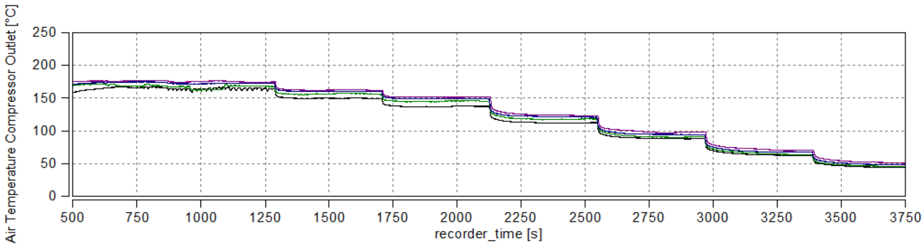

Figure 53: Air Temperature at Compressor Outlet.

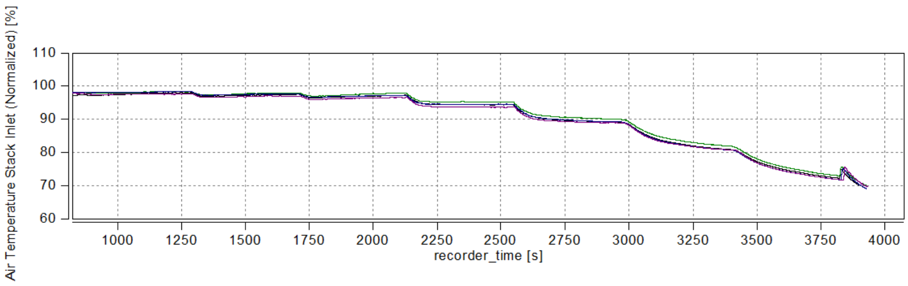

Figure 54: Air Temperature at Stack Inlet.

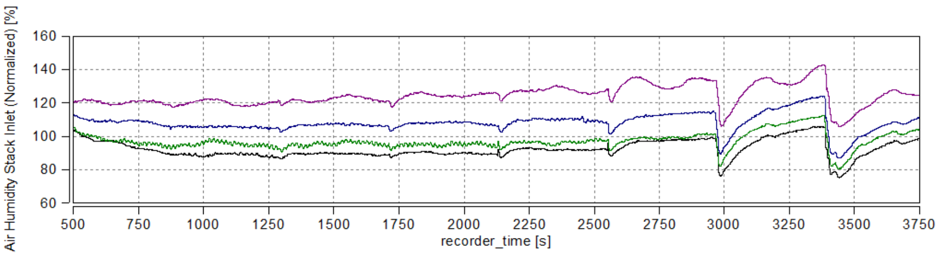

Figure 55: Air Humidity at Stack Inlet.

3.7 Fuel Cell System Durability Considerations

During the initial 1,000 hours of testing conducted within the framework of this project, the fuel cell stack degradation observed has exceeded the originally targeted limits. This deviation is primarily attributed to the nature of the ongoing development activities, which include frequent hardware modifications, system reconfigurations, and non-standard operating conditions that are not representative of steady-state or optimized commercial use.

The elevated degradation rates are not unexpected under such circumstances, as the test protocols employed often prioritize the evaluation of new control strategies, component integration, and transient operating scenarios over stack longevity. Consequently, certain stressors—such as repeated start-stop cycles, non-ideal

This project has received funding from the European Union's HORIZON EUROPE research and innovation programme under grant agreement No. 101096028. The content of this publication is the sole responsibility of the Consortium partners listed herein and does not necessarily represent the view of the European Commission or its services.

thermal and humidity management, and frequent off-nominal operation—have contributed to accelerated performance losses.

Despite these challenges, the degradation data collected thus far provides valuable insight into failure modes and operational sensitivities under development-centric conditions. These insights are being used to inform both hardware improvements and control strategy refinements.

In the upcoming phase of the project, we will implement and evaluate an improved online recovery procedure aimed at mitigating some of the reversible degradation mechanisms. This will include enhancements to purge protocols, optimized idle-time operation, and tailored recovery cycles designed to restore performance without interrupting standard operation.

As development stabilizes and the stack operating conditions become more representative of the target application, we anticipate a significant reduction in degradation rates. The results of the improved recovery procedure and subsequent testing will be documented in an amended version of this chapter, with updated performance metrics and degradation analyses.

This project has received funding from the European Union's HORIZON EUROPE research and innovation programme under grant agreement No. 101096028. The content of this publication is the sole responsibility of the Consortium partners listed herein and does not necessarily represent the view of the European Commission or its services.

4 Conclusion and next steps

The EMPOWER project has made significant strides in developing and validating innovative solutions for zero-emission heavy-duty vehicles (ZE HDVs). The project's primary focus was on the development and testing of the eAxle and Fuel Cell system, which are critical components in achieving competitive Battery Electric Vehicle (BEV) and Fuel Cell Electric Vehicle (FCEV) solutions. These efforts are essential for meeting the EU CO_2 targets and ensuring the market readiness of these vehicles by 2029.

The validation campaigns conducted under Work Package 2 (WP2) have demonstrated the robustness and reliability of the eAxle and Fuel Cell system. The comprehensive testing methodologies, including component-level testing, embedded software commissioning and calibration, functional validation, and durability and design verification testing (DVP), have ensured that these systems meet or exceed the required performance standards.

The eAxle validation included structural, lubrication, environmental, durability, and differential lock tests, which confirmed the system's ability to withstand real-world operational demands. Similarly, the Fuel Cell system underwent rigorous testing, including component validation, system integration, and performance assessment, to ensure its reliability and efficiency under various operating conditions.

Looking ahead, the next steps for the EMPOWER project will be the integration of the eAxle on both vehicles and the integration of a fuel cell in the FCEV; additionally both products will undergo further optimization and refinement under internal continuous improvement policy to enhance their performance and market readiness. In particular on the fuel cell development, the insights gained from the validation campaigns will inform future development efforts, ensuring that the final products meet the highest standards of quality and reliability. The project will continue to focus on achieving the EU CO_2 targets and delivering innovative solutions for zero-emission heavy-duty vehicles.

This project has received funding from the European Union's HORIZON EUROPE research and innovation programme under grant agreement No. 101096028. The content of this publication is the sole responsibility of the Consortium partners listed herein and does not necessarily represent the view of the European Commission or its services.

5 Bibliography

[1] "Greenhouse gas emissions from transport in Europe," [Online]. Available: https://www.eea.europa.eu/ims/greenhouse-gas-emissions-from-transport. [Accessed 20 09 2023].

[2] European Automobile Manufacturers' Association, "CO2 emissions from heavy-duty vehicles; Preliminary CO2 baseline (Q3-Q4 2019) estimate," March 2020.

[3] IEA Critical Minerals and Clean Energy Summit, "Electrification of road transport goes beyond cars and the ambition is growing," [Online]. Available: https://www.iea.org/energy-system/transport/trucks-and-buses. [Accessed 21 09 2023].

[4] European Automobile Manufacturers' Association, "Vehicles in use – Europe," January 2022.

This project has received funding from the European Union's HORIZON EUROPE research and innovation programme under grant agreement No. 101096028. The content of this publication is the sole responsibility of the Consortium partners listed herein and does not necessarily represent the view of the European Commission or its services.

6 Acknowledgment

European Union's HORIZON EUROPE research and innovation programme

This project has received funding from the European Union's HORIZON EUROPE research and innovation programme under grant agreement No. 101096028. The content of this publication is the sole responsibility of the Consortium partners listed herein and does not necessarily represent the view of the European Commission or its services.

Project Partners:

The author(s) would like to thank the partners in the project for their valuable comments on previous drafts and for performing the review.

Participant No*	Participant short name	Participant organisation name	Country
1 Coordinator	**AIT**	AIT Austrian Institute of Technology GmbH	AT
2	**IVECO**	IVECO SPA	IT
3	**FPT**	FPT Industrial SPA	IT
4	**IFPEN**	IFP Énergies nouvelles	FR
5	**POLITO**	Politecnico di Torino	IT
6	**LT**	Lead Tech SRL	IT
7	**VIL**	Villinger GmbH	AT
8	**CID**	Fundación CIDETEC	ES
9	**CTE**	CT Engineering GmbH	AT
10	**GLO**	GRUBER Logistics S.p.A.	IT
11	**BRE**	BREMBO SPA	IT
12	**IIT**	Istituto per Innovazioni Tecnologiche Bolzano S.c.a.r.l.	IT
13	**ALFI**	Air Liquide	FR